PERFORMANCE TEST OF NATURAL AND FORCED CONVECTION ON CLOSED LOOP PULSATING HEAT PIPE

Submitted By

Md. Majharul Islam Miraj

Student ID : BME1902018145

Md. Rakib Hossain

Student ID : BME1902018178

Md. Mamun Ur Rashid

Student ID : BME1902018224

Md. Mehadi Hasan

Student ID : BME1902018266

Supervised By

Md. Sojib Kaisar

Assistant Professor

SONARGAON UNIVERSITY

147/I, GREEN ROAD, PANTHAPATH, DHAKA

APPROVAL

The Thesis Entitled **"Performance test of natural and forced convection on closed loop pulsating heat pipe"** has been accepted as satisfactory for science in Mechanical Engineering approved as to its style and contents.

Submitted by

Md. Majharul Islam Miraj
ID- BME1902018145

Md. Mamun Ur Rashid
ID- BME1902018224

Md. Mehadi Hasan
ID- BME1902018266

Md. Rakib Hossain
ID- BME1902018178

Md. Sojib Kaisar

Assistant Professor

Department of Mechanical Engineering

Sonargaon University (SU)

147/I Green Rd, Dhaka 1215

ABSTRACT

With the advancement of science and engineering the need for space restricted cooling devices has increased. Closed loop pulsating heat pipe (CLPHP) is a new promising technology for heat transfer of microelectronics. In it by simple mechanism heat is transferred effectively and efficiently. The combination of processes like bubble nucleation, collapse, formation of vapor plugs and slugs, agglomeration, dynamic instabilities and temperature/pressure perturbation, etc. leads to exceptional heat transfer capability of the heat pipe. The aim of this research paper is to better understand the operation of PHP through experimental investigations and obtain comparative results for different parameters. A series of experiments are conducted on a closed loop PHP (CLPHP) with 6 loops made of copper capillary tube of 2 mm inner diameter. The heat pipe structure is using normal, CLPHP. Ethanol, DI Water and Ethylene Glycol is taken as the working fluid. The operating characteristics are studied for the variation of heat input, filling ratio (FR) and orientation. The single filling ratios are 25%, 50%, 75% based on its total volume. Natural Convection and Forced Convection are measure this. This paper attempts to demonstrate the effect of variation of different parameters on the same structure as well as the variation of thermal performance depending on the presence of wire insert and fins on different structures.

ACKNOWLEDGEMENT

This is to place on record our appreciation and deep gratitude to the faculty members, without whose support this project would have not ever seen the light of day. We have immense pleasure in expressing our gratitude to our supervisor, Md. Sojib Kaisar, Assistant Professor, Department of the Mechanical Engineering, his guidance, insightful suggestions encouragement, and for all facilities to complete this project. We express their profound thanks to him for everything he done.

We also like to thanks the lab assistants from “Heat Transfer lab” at Sonargaon University, for their assistance in setting up the project work and lending their time and expertise to finish our experiment.

Finally, we would want to express our gratitude to everyone who helped us in any way to finish the thesis.

Table of Contents

List of Figures

List of Table

NOMENCLATURE

R_{th}	= Thermal resistance (°C /W)
Q	= Heat input (W)
ρ	= Density (Kg/m3)
V	= Specific Volume (m3/kg)
T_e	= Evaporator Temperature (°C)
T_c	= Condensation Temperature (°C)
ΔT	= Temperature difference (°C)
C_P	= Specific Heat (kJ/Kg-K)
D	= Diameter (mm)
D_i	= Inner Diameter (mm)
D_o	= Outer Diameter (mm)
h	= Heat transfer Co-efficient (W/K-m^2)
L	= Length (mm)
W	= Watt
PHP	= Pulsating Heat Pipe
CLPHP	= Closed Loop Pulsating Heat Pipe
FR	= Filling Ratio (%)

1 CHAPTER - INTRODUCTION

1.1 Introduction

With the advancement of modern society, the need for miniaturization and compactness has increased. Entire human civilization now opts for smart and convenient devices that are easy to carry and user friendly. Everyday latest versions of existing electronics are being launched and new designs are being fabricated. This has brought the present society face to face with problems of high-power dissipation and heat density. Market demand for efficient microelectronics has posed the challenge of thermal management of increased power levels coupled with high heat fluxes. To mitigate and solve this problem of power electronics, the use of liquid-vapor phase change cooling devices such as the heat pipes, have been introduced. Although the conventional heat pipes (e.g. mini or micro) are one of the proven technologies, the manufacturing of the complex, miniaturized wick structure/geometry of these heat pipes could become the most cost intensive factor. Another common limitation is the capillary limit, which occurs when the wick structure cannot return an adequate amount of liquid back to the evaporator. With a view to overcome these difficulties researchers have come up with pulsating heat pipes (PHP) which work on the principle of oscillation of the working fluid and phase change phenomenon in a capillary tube. PHP is a meandering tube of capillary dimensions with many turns filled partially with a suitable working fluid with no wick structure. PHPs are passive two-phase thermal control devices first introduced by Akashi et al [1-4]. In this application, reduced diameter channels are used, which are directly influenced by the selected working fluid. The vapor plugs generated by the evaporation of the working fluid push the liquid slugs toward the condensation section and this motion causes flow oscillations that guide the device operation [5]. Performance of a PHP depends upon many factors like the geometrical parameters of flow channel, the working fluid, the filling ratio, and number of turns, PHP configuration and the inclination angle [5]. Toe purposes of this investigation are to study the heat transfer characteristics of an CLPHP and evaluate several issues related to its performance. There are many engineering practical situations where heat is being transferred under conditions of pulsating and reciprocating flow such as the operation of modem power producing facilities and industrial equipment used in metallurgy, aviation, chemical and food technology. Cavitation’s in hydraulic pipelines, pressure surges and flow of blood are also some of familiar instance of such flows. The performance of this equipment in thermal engineering application is affected by the pulsating flow parameters (Al-Had-dad and Al-Binally, 1989). During the past few decades, numerous studies have been devoted to this pulsating flow and its associate heat transfer problems. A review of these studies with emphases on the onset of turbulence, velocity distribution and pipe flow as well as the heat transfer characteristics including axial heat transfer enhancement and convective heat transfer are presented in the following section.

1.2 Heat Pipe

Heat Pipe Technology (HPT) was founded in 1983 with a grant from the Department of Energy for a project to begin research on new uses for heat pipe technology. Heat pipes are tubes that have a capillary wick inside running the length of the tube, are evacuated and then filled with a refrigerant as the working fluid and are permanently sealed. The working fluid is selected to meet the desired temperature conditions and is usually a Class I refrigerant. Fins are similar to conventional coils - corrugated plate, plain plate, spiral design. Tube and fin spacing are selected for appropriate pressure drop at design face velocity. Heating, Ventilation, and Air Conditioning (HVAC) systems typically use copper heat pipes with aluminum fins; other materials are available.

The heat pipe is one of the remarkable achievements of thermal physics and heat transfer engineering in this century because of its unique ability to transfer heat over large distances without considerable losses. The main applications of heat pipes deal with the problems of environmental protection and energy and fuel savings.

Heat pipes enable passive cooling solutions for high heat load and high temperature equipment, lacking moving parts and boasting extraordinary lifetimes as a result. The idea of heat pipe was given by Gaugler [6] from General Motors. However, the technology of that period presented no clear need for such a device and it lay dormant for two decades. Then it was in 1963 when a Los Alamos National Research Laboratory engineer named George Grover [6] demonstrated the first heat pipe. Heat pipe technology was borrowed from simple heat conducting pipes used by English bakers 100 years ago. Since 1963, heat pipes progressed and modem applications of this technology range from miniature heat pipes for cooling processors inside laptop computers, to groups of half inch diameter and five feet long pipes that will be used in NASA spacecraft, to pipes of two inches diameters (or more) which are used to cool injection molds used in plastic forming. The lengths of the pipes can vary from inches to 24 feet or more.

Starting in the 1980s Sony began incorporating heat pipes into the cooling schemes for some fits commercial electronic products in place of both forced convection and passive finned heat sinks. Initially they were used in tuners and amplifiers, soon spreading to other high heat flux electronics applications.

1.3 Closed Loop Pulsating Heat Pipe

Pulsating Heat Pipes (PHPs) are a passive heat transfer device and do not require a pump or additional power to operate. They also do not need a wicking structure to transport the liquid and can work at higher heat fluxes. Heat transfer is through natural oscillations of the working fluid between the evaporator and condenser sections. PHPs consist of a long meandering tube which is heated and cooled at various points along its length. Their operation is based on the principle of oscillation for the working fluid and a phase change phenomenon in a capillary tube. The diameter of the tube must be small enough such that liquid and vapour plugs exist.

Initially, the PHP is evacuated and then partially filled with the working fluid. Effects from surface tension cause the formation of liquid slugs interspersed with vapour bubbles. As heat is applied to the evaporate section, the working fluid begins to evaporate. These results in an increase of vapour pressure inside the tube which causes the bubbles in the evaporator zone to grow and pushes the liquid towards the condenser. As the condenser cools, the vapour pressure reduces and condensation of bubbles occurs. This process between the evaporator and condenser section is continuous and results in an oscillating motion within the tube. Heat is transferred through latent heat of the vapour and through sensible heat transported by the liquid slugs. When one end of the bundle of turns of the undulating capillary tube is subjected to high temperature, the working fluid inside evaporates and increases the vapour pressure, which causes the bubbles in the evaporator zone to grow. This pushes the liquid column toward the low temperature end (condenser). The condensation at the low temperature end will further increase the pressure difference between the two ends. Because of the interconnection of the tubes, motion of liquid slugs and vapour bubbles at one section of the tube toward the condenser also leads to the motion of slugs and bubbles in the next section toward the high temperature end (evaporator). This works as the restoring force. The inter-play between the driving force and the restoring force leads to oscillation of the vapour bubble and liquid slugs in the axial direction. The frequency and the amplitude of the oscillation are expected to be dependent on the shear flow and mass fraction of the liquid in the tube.

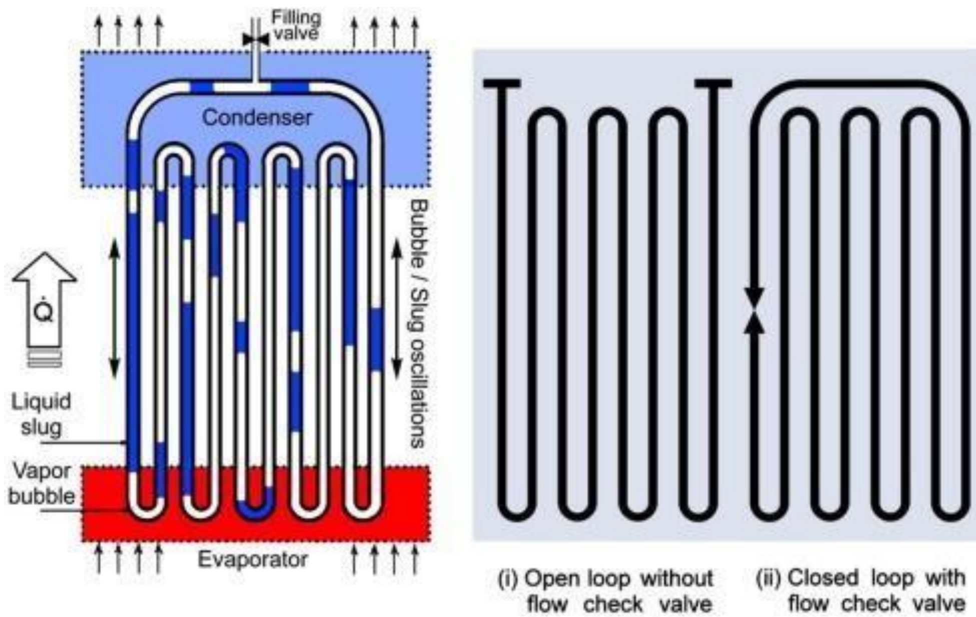

Figure 1.1 Model of CLPHP

Recently, Holley and Faghri [13] and Zuo et al. [14] [15] prototyped and studied PHPs using a sintered metal wick. Both heat transmission and liquid dispersion should be aided by the wick. A PHP must have at least one area that is heated and another that is cooled. The capillary tube's bends are often where the evaporators and condensers are situated. A working fluid is first partly injected into the tube after it has been emptied. As liquid slugs and vapor bubbles, the liquid and its vapor will be dispersed throughout the pipe. The bubbles in the PHP's evaporator portion will see a rise in vapor pressure as it warms up. This pushes the liquid slug towards the direction of the heat pipe's condenser portion. The vapor bubbles will start to condense as they get to the condenser. Vapor pressure falls when the vapor transitions phases, causing the liquid to return to the condenser end. In this manner, the PHP is configured to have a constant oscillating flow. New vapor bubbles will also arise as a result of boiling the working fluid. There are two types of research on PHPs: experimental and theoretical. While experimental research has concentrated on either defining the heat transfer or visualizing the flow pattern in PHPs.

B.Y Tong, et al, [16] conducted flow visualization for the closed loop PHP using a charge coupled device (CCD). It was observed that during the start-up period, the working fluid oscillates with large amplitude, however, at steady operating state, the working fluid circulates. The direction of circulation for the working fluid is consistent once circulation is attained, but the direction of circulation can be different for the same experimental run. It was also concluded that large amplitude oscillations from the evaporator to the condenser occur in the closed loop PHP during the startup period. After this period, continuous circulation in the working fluid occurs. When the working fluid is circulating, the slugs also experience local oscillations.

1.4 Parameters affect the performance of CLPHP

Advancement is taking place in every field of engineering and increasing the demand of smaller and effective heat transfer devices. This leads to the development of Pulsating Heat Pipe (PHP). PHP is a passive two-phase heat transfer device for handling moderate to high heat fluxes typically suited for power electronics and similar applications. It usually consists of a small diameter tube, closed end-to-end in a loop, evacuated and then partially filled with a working fluid. The internal flow patterns in a PHP are a function of the applied heat flux. This paper highlights the thermo-hydrodynamic characteristics of these devices. State of art indicates that at least three thermo-mechanical boundary conditions have to be met for the device to function properly as pulsating heat pipe. This includes internal tube diameter, applied heat flux and filling ratio. Additionally the numbers of turns and thermo-physical properties of working fluid also play a vital role in determining the thermal behavior. Apart from this, paper is a literature review on pulsating heat pipe technology; work performed by researchers. Finally, unresolved issues on the mechanism of PHP operation with different type of working fluids, validation techniques and applications are discussed.

1.5 Operational Conditions: Ratio of filling:

The volume percentage of the heat pipe that is first filled with liquid is known as the filling ratio. When the maximal heat transfer rate is realized at a certain temperature, the ideal filling ratio is ascertained experimentally.

1.6 Dry-out Conditions

This issue limits how well heat pipes can work. When all of the working liquid has evaporated and the region around the evaporator is completely dry, we may say that a dry out situation has occurred. Low filling percentage results in this situation and the pipe receives a lot of heat input. When a dry situation is reached, conduction is the only mechanism through which heat exchange occurs.

1.7 Convectional Heat Transfer

Convection is a significant way of mass transport in fluids and one of the main kinds of convective heat transfer. Both advections, in which matter or heat is transferred by the larger-scale motion of currents in the fluid, and diffusion, the random Brownian motion of individual particles in the fluid, are mechanisms for convective heat and mass transmission. Convection is the word used to describe the combination of advective and diffusive transfer in the context of heat and mass transport. The word "convection" is often used to refer broadly to the convection process, heat transmission by convection as opposed to mass transfer by convection. As contrast to "forced heat convection," which occurs when forces other than buoyancy (such as a pump or fan) move the fluid, "free heat convection" (natural heat convection) is caused by temperature-induced changes in buoyancy. The term "convection" should only be used in its broadest meaning in mechanics, and for the sake of clarity, distinct forms of convection should be distinguished. Based on driving power, convection may be divided into two categories:

• **Natural convection**: This phenomenon is brought on by temperature variations that alter the density and therefore the relative buoyancy of the fluid. Bulk fluid flow results from the movement of heavier, denser components falling and lighter, less dense ones rising. Therefore, natural convection can only happen in a gravitational field. The Rayleigh number may be used to identify when natural convection begins (Re).

• **Forced/Active convection**: Also known as heat advection, this kind of convection occurs when external surface forces, like a fan or pump, are applied. Usually, forced convection is utilized to speed up heat transfer. The Nusselt Number may be used to calculate the ratio of convective to conductive heat transfer across the boundary (Nu).

1.8 Evaporator Section

In the evaporator section of the heat pipe the working fluid absorbs heat from the heat source. It is located on the bottom section of the heat pipe. Heat is supplied to the heat pipe using Nichrome wire connected to a variable power supply. The Nichrome wire is wound around the pipes in the evaporator section on top of a layer of mica tape. The mica sheet prevents direct contact of copper tube with Nichrome wire to prevent any possibility of short circuit connection. The evaporator section is further enveloped by asbestos sheet to reduce heat loss to the environment.

1.9 Adiabatic Section

It is located between the evaporator section & condenser section. In here the liquid & vapor phases of the fluid flow in opposite directions and no significant heat transfer occurs between the fluid & surrounding medium. The part of the tube in adiabatic section is wound with aluminum foil paper, glass wool and finally covered with heat insulating tape to prevent heat transfer to the surrounding environment.

1.10 Condenser Section

It is the section of the heat pipe where heat is rejected from the working fluid to the surrounding. In this section, the working fluid condenses & rejects the same amount of heat which is absorbed from the evaporator section. In this experiment, this section is located on upper section of the heat pipe and a AC fan help dissipation of heat continually.

1.11 CLPHP Limitations

The rate of condensation and evaporation is the only factor affecting how quickly heat is transferred through the heat pipe.

• **Capillary Limit**: This condition arises when the capillary pressure is insufficient to transfer enough liquid from the condenser to the evaporator. leads in the evaporator to dry out. Dry out makes it impossible for the thermodynamic cycle to continue, and the heat pipe stops working correctly.

• **Boiling Limit**: this condition develops when the liquid in the wick boils and evaporates, leading to dry out. It is brought on by radial heat flux into the heat pipe.

1.12 Motivation

The Motivation for this research comes basically from the need of a compact thermal management system suitable for the present blossoming technology-based civilization. One of the most important technologies in the development of electronic products is thermal management, and this trend will continue. The limitations of design are always being pushed, and current trends in thermal management of electronics are quite demanding. Inferred from a market analysis is that the following products are in demand.

1.13 Objectives

This thesis work is designed with the aims with following objectives:

I. To investigate the thermal performance of CLPHP with three different working fluids (Distilled Water, Ethanol and ethylene glycol) for natural convection.
II. To investigate the thermal performance of CLPHP with three different working fluids (Distilled water, Ethanol and ethylene glycol) for forced convection.
III. To compare the effect of convection type in CLPHPs for different filling ratios.
IV. To gain a optimum filling ratio after comparison.

2 CHAPTER - LITERATURE REVIEW

2.1 LITERATURE REVIEW ON PULSATING HEAT PIPES

While our area of interest lies in the two-phase regime, it is worthwhile to mention briefly about relevant studies in pulsating/oscillating single phase flows. Experimental and numerical analyses of such flows require more stringent time and spatial resolutions, and therefore there exist fewer investigations of oscillatory flow heat/ mass transfer. In general, oscillatory flows can be grouped into two-categories: pulsating (modulated) and reciprocating (fully reversing) flows. Pulsating flows are always unidirectional and can be decomposed into steady and unsteady components. For reciprocating flows, the flow direction cyclically changes. Hence these flows convect zero net mass flow. Fundamental and applied studies on pulsating and reciprocating single phase flows have been performed among others by Siegel and Pearlmutter [1962], Kurzweg and Zhao [1984], Zhao and Cheng [1995] and more recently by Sert and Beskok [2003].

PHPs have advantages with respect to their simple structure, fast thermal response, higher heat transfer rate, and simple construction, and they have applications in heat recovery systems, electronic cooling systems, space, cryogenic, automobiles, solar and thermal energy, among others [16–17]. PHPs have two main sections called the evaporator and condenser sections, and their performance relies on the oscillatory/pulsatory mode of the internal working fluid between these two sections. The evaporator section is the heating section where the evaporation of liquid film or flow boiling occurs, while the condensation of the two-phase flow occurs in the condenser section. The internal complex flow patterns, ranging from the slug-plug flow to annular flow, are initiated by the interior pressure instabilities of alternative tubes, which affect the total heat flux from the evaporator to condenser sections [10]

The performance of the PHPs is affected by various parameters, including its structure, working fluid, operating environment, outer diameter, number of turns, total height, filling ratio, inclination angle, and condenser area [17–19]. The gravitational force also plays an important role with respect to the use of PHPs for space applications. Ayel et al. [15] performed an experimental study on the effect of various gravity forces on closed-loop PHP (CLPHP), and they concluded that these heat pipes continue to operate even in microgravity conditions, and the thermal performance is enhanced when operated in a vertical orientation. Recently, the operating temperature effect was also investigated for cryogenic PHPs that can operate at very low temperatures (4 K–77 K). Fonseca et al. [16] designed a helium-based cryogenic PHP, where the oscillation period starts within the time range of 21 s only. The research on cryogenic PHPs is further extended by using hydrogen, neon, and nitrogen as a working fluid for engineering-based applications [17–19].

2.2 LITERATURE REVIEW

Pulsating Heat Pipes (PHPs) has been the subject of research in an increasing number of laboratories m the recent times. PHPs were presented in 1971 by Smyrnov in a Russian Patent and in 2003 in a U.S. patent. PHP in the form as they are investigated today have been first proposed by Akachi [1-4] in the 1990.

P. Charoensawan et.al [8]; studied the effect to CLPHP thermal performance depends on various parameter like internal diameter of tube, number of turns, working fluid and inclination angle of the device and experimentally studied. The conclusion of P. Charoensawan's experimentation were, gravity has a great influence on the performance on the CLPHP, internal diameter must be specified with critical Bond number within the limit, the performance can be increased by increasing the ID and/or no. of meandering turns, the buoyancy forces effect bubble shape. Different fluids are beneficial under different operating conditions and the relative share of latent beat and sensible heat, flow behaviour.

Honghai Yang et.al. [9] presented a paper on experimental study on the operational limitation of closed loop pulsating heat pipes (CLPHPs). investigated, viz. vertical bottom flux on thermal performance and performance limitation were investigated. The CLPHPs were operated till performance limit characterized by serious evaporator overheating (dry- out) occurred. Rather high heat loads could be accommodated. An experimental study was pe formed on tow closed loop pulsating heat pipes (CLPHPs) to investigate the effects of inner diameter, filling ratio, operational orientation and heat toad on thermal performance and occurrence of performance limitation in the form of evaporator dry-out. In general, the CLPHPs obtain the best thermal performance and maximum performance limitation when they operate in the _vertical bottom heat mode with 50% filling ratio. As the inner diameter decreases, performance differences due to the different heat modes (i.e. the effect of gravity) become relatively small and even insignificant. The effect of inner diameter and inclination angles on operation limit of a closed loop oscillating heat pipes with check valves (CLOHP/CV) were studied in this paper. Copper tubes of ID 1.77 and 2.03 mm with 10 turn, with Rl23 was used as the working fluid. The inclination angles were 0°.

P. Meena et al. [10] were concluded that when the inner diameter changed from 1.77-2.03 mm the critical temperature increased. And when increase the inclination angles from O until to 90° the critical temperature increased.

S. Rittidech et.al. [11] a visualization study of the internal flow patterns of a closed-loop oscillating heat-pipe with check valves (CLOHP/CV) at normal operating condition for several evaporator lengths (Le), and ratio of check valves to number of turns (Rev) has been conducted. This article describes the effects of varying Le, and Rev on flow patterns. It was found that the internal flow patterns could be classified according to the Le and Rev as follows: At the high heat source when the Le decreases the main flow changes from the bubble flow with slug flow to disperse bubble flow. The Rev decreases the main flow changes from the disperse bubble flow with bubble flow to disperse bubble When the velocity of slug increases, the length of vapor bubbles rapidly decreases and the heat flus rapidly increases. The ratio of check valves to number of turns decreases the main flow changes from the dispersed bubble flow with bubble flow to disperse bubble flow for the high heat source.

P. Meena, et.al. [12] has aims to study the effect of evaporator section lengths and working fluids on operational limit of closed loop oscillating heat pipes with check valves (CLOHP/CV). It is experimentally concluded when the evaporator lengths increased the critical heat transfer flux decreased. There was working fluids change from R123 to Ethanol and water the critical heat flux decreased. The latent heat of vaporization affects the critical heat flux. The working fluid with the lower latent heat of vaporization exhibits a higher critical heat flux.

Stephane Lips Ahlem Bensalem et al. [13] various experiments were conducted on two full size pulsating heat pipes (PHP) which differed from their diameter, number of turns, and working fluid. The analysis of the experimental results for low heat fluxes the PHP performance is sensitive to the orientation and for high heat fluxes, it is independent from the orientation. The experiments were conducted at the scale of a single branch of a PHP. The test section was either adiabatic or heated. The adiabatic experiments brought to therefore the importance of dynamic contact angles in the flow and the dissymmetry between the

N. Panyoya et al. [14] the purpose of this research was to determine the effects of aspect r ratios (ratio of evaporator length to the inner diameter of tube) and number of meandering turns on performance limit of an inclined closed-loop oscillating heat pipe. The geometrical sizes, which were the variable parameters were the internal diameter, the evaporator section length of, the adiabatic and condenser section length of each set was equal to the evaporator length and the numbers of meandering turn and also variable inclination angles adjusted by 10°.The result indicated that the aspect ratio, the ratio of evaporator length by internal diameter and number of meandering turns significantly affect the maximum heat flux and inclination angle. The effects of aspect ratios and number of meandering turns on maximum heat flux of an inclined CLOHP have been thoroughly investigated in this study. In the case of aspect ratio, it can be seen that, the highest maximum heat flux occurs at inclination angle about 70-90° and lower value of aspect ratio. In the case of number of meandering turns, it can be seen that, when number of meandering turns increases, number of meandering turns does not affect to the maximum heat flux. In the case of inclination angle, it can be seen that, when the inclination angle increases from 0-90°, the maximum heat flux increases with respect to increasing numbers of tubes. Moreover, the highest maximum heat flux occurs at vertical position to about 70°. P. Sakulchangsatjatai et al. [15] this research studies the effect of length ratios on heat transfer characteristic of Closed Loop Oscillating Heat Pipe with Non-Uniform Diameter (CLOHP/NUD) 1.e. inner diameter of capillary tube were alternated connection and bent into several numbers of turns and both ends were connected to form of loop. It was found that, the CLOHP/NUD transferred higher heat than the conventional Closed Loop Oscillating Heat Pipe (CLOHP) with the same heat transfer area because the working fluid flowed in only one direction. Working fluid moved to condenser section in larger inner diameter and returned to evaporator section in smaller inner diameter. The heat transfer performance of CLOHP/NUD can be improved if one directional circulation of working fluid can be induced. The effects of length ratios and working fluids on the heat performance of CLOHP/NUD have been experimentally investigated and conclude heat flux increased when the length ratio decreased.

3 CHAPTER - EXPERIMENTAL SETUP & PROCEDURE

3.1 View of Experimental Set Up

For the purpose of researching the heat transfer properties of a closed loop pulsating heat pipe, an experimental facility has been designed, built, and put into operation. This chapter presents a thorough description of the experimental setup and methodology.

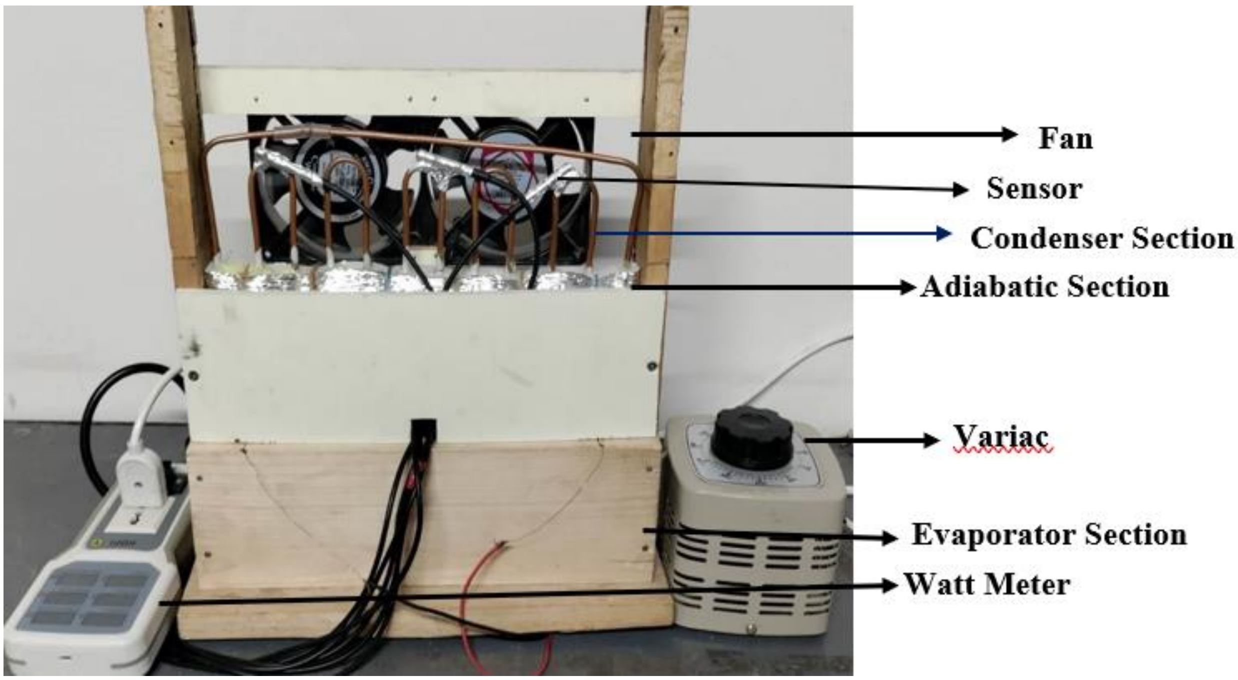

Figure 3.3.1 Experimental Set Up of CLPHP

3.2 Experimental Equipment & Working Fluid

An experimental facility has been designed, fabricated and installed to collected data for this research. The detailed description of experimental apparatus and experimental procedure are presented in this chapter.

Thus, apparatus used in this experiment are-

- Pulsating heat pipe
- Ethanol
- Ethylene glycol

- Distilled Water
- Test stand
- Variable power supply
- Nichrome Wire
- Aluminum Foil Paper
- Glass wool
- Foam tape
- Coper Capillary Tube
- Silicon Tube
- Watt Meter
- Electric Wire
- AC fan
- Asbestos tape
- Temperature Sensor (DS18B20)
- Arduino Mega
- Arduino 1.5.2 Compiler
- Syringe
- Data Acquisition System (DAQ) – PLX-DAQ

3.3 Dimension of our Experimental CLPHP Model

A closed loop pulsating heat pipe or oscillating heat pipe consists of a metallic tube of capillary dimensions wound in a serpentine manner & joined end to end. It consists of sections. They are:

- Evaporator section 50 mm of CLPHP tube.
- Adiabatic section 100 mm of CLPHP tube.

•	Condenser Section 60 mm of CLPHP tube.

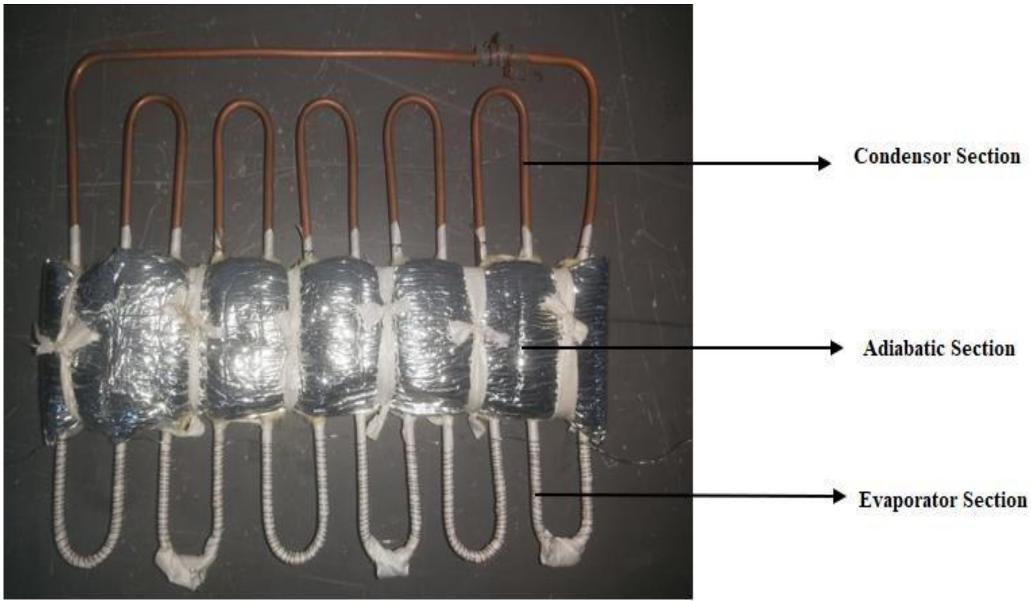

Figure 3.2 Schematic of Experimental CLPHP Model

3.4 Working Fluid

Here is the use of Ethanol, Ethylene glycol and Distilled Water as a working fluid.

3.4.1 **Distilled Water**

Water that has been heated into vapor and then condensed back into liquid in a different container is known as distilled water. The original container still contains any impurities in the original water that do not boil at or below the boiling point of water. So, one kind of cleansed water is distilled water.

Figure 3.3 Distilled Water

3.4.2 **Ethanol**

Commonly referred to simply as alcohol or spirits, ethanol is also called ethyl alcohol, and drinking alcohol. It is the principal type of alcohol found in alcoholic beverages produced by the fermentation of sugars by yeasts. It is a neurotoxic psychoactive drug and one of the oldest recreational drugs used by humans. It can cause alcohol intoxication when consumed in sufficient quantity. Ethanol is used as a solvent, an antiseptic, a fuel and the active fluid in modem (post-mercury) thermometers. It is a volatile, flammable, colorless liquid with a strong chemical odor. Its structural formula CH3CH2OH, is often abbreviated as C2H5OH or C2H6O.

Figure 3.4 Ethanol

3.4.3 **Ethylene Glycol**

Ethylene glycol, also called ethane-1,2-diol, the simplest member of the glycol family of organic compounds. A glycol is an alcohol with two hydroxyl groups on adjacent carbon atoms . Ethylene glycol is a clear, sweet, slightly viscous liquid that boils at 197.3 °C (388.4 °F). Its most common use is as an automotive antifreeze.

Figure 3.5 Ethylene Glyco

Table 3.1 Properties of Working Fluids

Sl	Parameters	Distilled Water	Ethanol	Ethylene Glycol
1	Melting point	0°C	-114.1°C	-12.9°C
2	Boiling point	100°C	78.23°C	197.3°C
3	Density	997 kg/m^3	0.79 g/cm^3	1.1132 g/cm^3

3.5 Test Stand

The test stand is a wood structure. The whole structure is supported by two columns which is situated in a large wood base.

Figure 3.6 Experimental test stand

3.6 Heating Apparatus

Heating apparatus can be used to transfer heat. It is used for heat transfer from one place to another.

3.6.1 Variable power supply

Variable power supply provides variable voltage to run different types of operations or the operation that requires different voltage in times. We used voltages ranges from 20-60 volts by this power sources. It is connected to the power supply unit to provide variable power (beat input) by varying voltage output.

Figure 3.7 Variac

Table 3.2 Specifications of variable power supply

Phase	3ϕ
Rated capacity	300 volt
Rated frequency	60Hz
Input voltage	220 volt

3.6.2 Nichrome wire

Nichrome wire is an al1oy typically made of 80 percent nickel and 20 percent chrome. Because of Nichrome wire’s high internal resistance, it heats up rapidly when applying electricity and also cools rapidly when shut off or removed from a heat source. It maintains Its strength as the temperature rises and has a higher melting point than other wire. It does not oxidize or corrode, and is non-magnetic and highly flexible.

Figure 3.8 Nichrome wire

3.6.3 Watt Meter

The wattmeter is an instrument for measuring the electric active power (or the average of the rate of flow of electrical energy) in watts of any given circuit. Electromagnetic watt meters are used for measurement of utility frequency and audio frequency power; other types are required for radio frequency measurements.

3.6.4 Electric Wire

To conduct the flow of electricity, we used electric wire of negligible diameter. Heat sensing element that combines LM35 required electric wire to receive and supply data through electricity.

3.7 Insulating Materials

Material that is used to stop the passage of electricity, heat, or sound from one conductor to another.

3.7.1 Aluminum Foil

For the insulation of pulsating heat pipe, aluminum foil tape is used. It resists flame, moisture, temperature extremes, UV exposure and most chemicals with a backing that withstands harsh environments. We used metal-backed foil tapes with the conformability to wrap tightly around virtually any shape or contour. With the used of this aluminum foil tape, we managed to resist heat loss during temperature measurement in different voltage was in run.

3.7.2 Glass wool

Glass wool is an insulating material made from fibers of glass arranged using a binder into a texture similar to wool. The process traps many small pockets of air between the glass, and these small air pockets result m high thermal insulation properties. It reduces the beat loss and is used as insulator.

3.7.3 Heat insulating Foam Tape

This is used as a heat insulator and the adhesive side of the tape helps to bind the glass wool in the adiabatic section.

Figure 3.9 Foam Tape

3.7.4 Silicon Tube

Silicone tubing is a tough elastomer. Flexible but strong, the tubing is a vital material across a broad range of industries. The material's resistance makes it suitable for lots of different devices, but some important properties make it particularly useful in healthcare and pharmaceutical sectors.

3.7.5 Asbestos Tape

Typically, it is used for thermal insulation. Duct tape was designed to be used for taping different types of ducts, notably those used for heating. Its name, which everyone has grown to know and love, derives from this highly useful purpose. The tape prevents heat from escaping, making it a practical and cost-effective device. Duct tape has evolved into a popular household item with many applications. It is available in a wide range of hues, sizes, and degrees of quality. We utilized 2" wide by.25" thick asbestos tape for our experiment.

Figure 3.10 Asbestos tape

3.7.6 Temperature Sensor (DS18B20)

The DS18B20 is an integrated circuit sensor having a temperature-dependent electrical output that may be used to monitor temperature (in ^{o}C). Six sensors in all are attached to the pulsing heat pipe's wall: three for the evaporator part and the remaining three for the condenser section.

To measure temperature, they are calibrated and attached to various heat pipe segments. It is inexpensive and, as a result of its popularity, is offered in a variety of probes. The best advantage of employing the sensors is obtained by integrating them with the Arduino microcontroller to get precise data and readings using programming language.

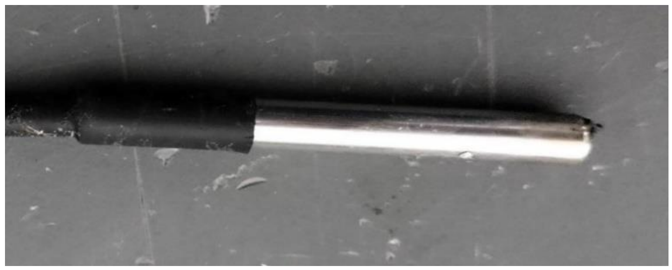

Figure 3.11 Temperature Sensor (DS18B20)

3.7.7 Arduino Mega

A microcontroller board called the Arduino Mega is based on the ATmega2560 (datasheet). It contains 16 analog inputs, 4 hardware serial ports, a 16 MHz crystal oscillator, 54 digital input/output pins, 15 of which may be utilized as PWM outputs, a USB port, a power connector, and an analog input. A reset button and an ICSP header. It comes with everything required to support the microcontroller; to get started, just plug in a USB cable, an AC-to-DC converter, or a battery. The majority of shields made for the Arduino Duemilanove or Diecimila are compatible with the Mega.

3.7.8 Data Acquisition System (DAQ) PLX-DAQ

PLX-DAQ is a Parallax microcontroller data acquisition add-on tool for Microsoft Excel. Any of our microcontrollers connected to any sensor and the serial port of a PC can now send data directly into Excel.

3.8 AC Fan

AC fans are the fans that are powered by alternating sinusoidal electric current. These fans are powered by positive current and the same amount of negative current. The general frequencies of AC voltage for the AC fans are 100 volts, 120 volts, 200 volts, 220 volts, 230 volts, and 240 volts at max.

3.9 EXPERIMENTAL PROCEDURE

For Close Loop Pulsating Heat Pipe experiment, make a wooden platform for set up experimental equipment. Then there adjust fans. For experiment, bend 2 mm inner dia heat pipe was evaporator section 50 mm, adiabatic section 100 mm and condenser section 60 mm with parallel pipe distance 20 mm. Then connected arduino sensor with evaporator and condenser section and insulated it. Then twist nichrome wire and insulated it. Then whole apparatus put up to the wooden platform. Then connect power supply so that the program may run and the appropriate data readings can be taken. In the experiment the heat transfer characteristics were measured for three different fluids as distilled water, Ethanol, Ethylene glycol with different fluid ratio. Also, the characteristics were measured for natural convection and forced convection. For dry the heat pipe sealed out at bottom and top side and provide heating. After some time stop heating and start cooling by fan. After cooling this, injected the distilled water with proper ratio and sealed it top and bottom side by the silicon tube. Then provide heat at selected power by variac, then record data with arduino. Natural convection and forced convection both system measure data. Then increase selected power supply one by one and take data and also change fluid ratio. The technic described above was continued, with the filling ratio subsequently, For the working fluids ethanol and ethylene glycol, respectively.

4 CHAPTER - RESULT AND DISCUSSIONS

4.1 Experiment conducted for DI water 25% (Natural Convection)

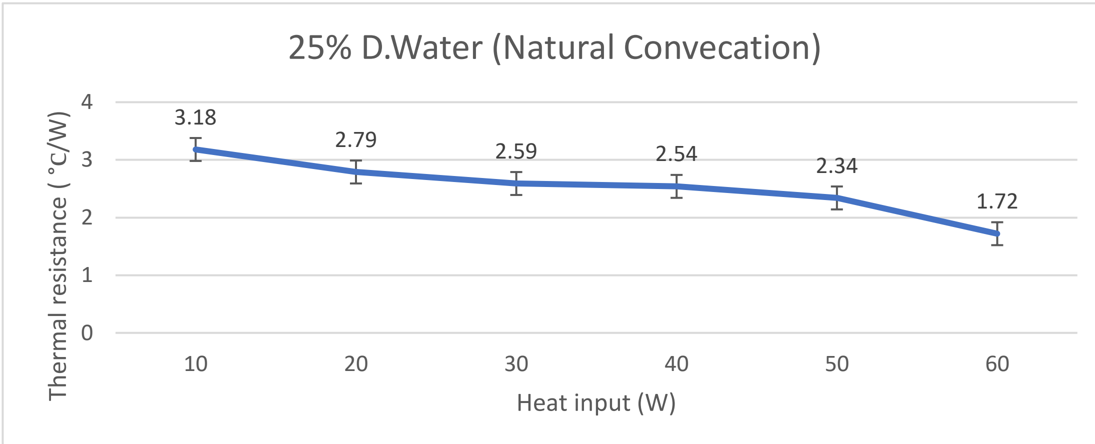

Figure 4.1.1 Thermal Resistance vs Heat input for Distilled water 25% (N. C)

In Fig. 4.1.1, It is noticed that the thermal resistance is decreasing with increment of heat input. In addition, if it is seen more closely, the thermal resistance moves down in between 10W to 30W and stayed almost same up to 40W. However, it goes down after that point.

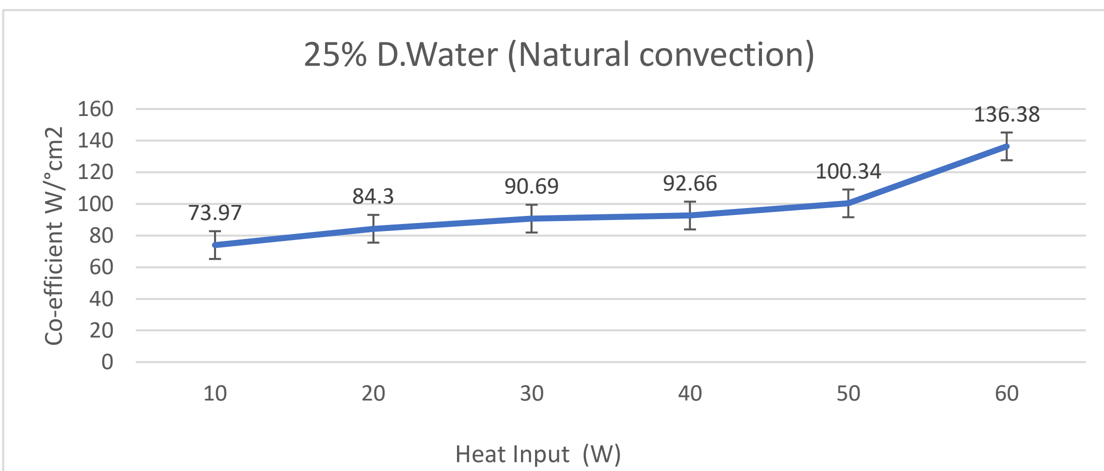

Figure 4.1.2 Thermal Co-Efficient vs Heat Input for 25% DI water (N. C)

In Fig. 4.1.2, It is noticed that the thermal co-efficient is increasing with decrement of heat input. In addition, if it is seen more closely, thermal co-efficient moves up in between 10W to 30W and stayed almost same up to 40W. however it goes up after that point.

4.2 Experiment conducted for DI water 25% (Forced Convection)

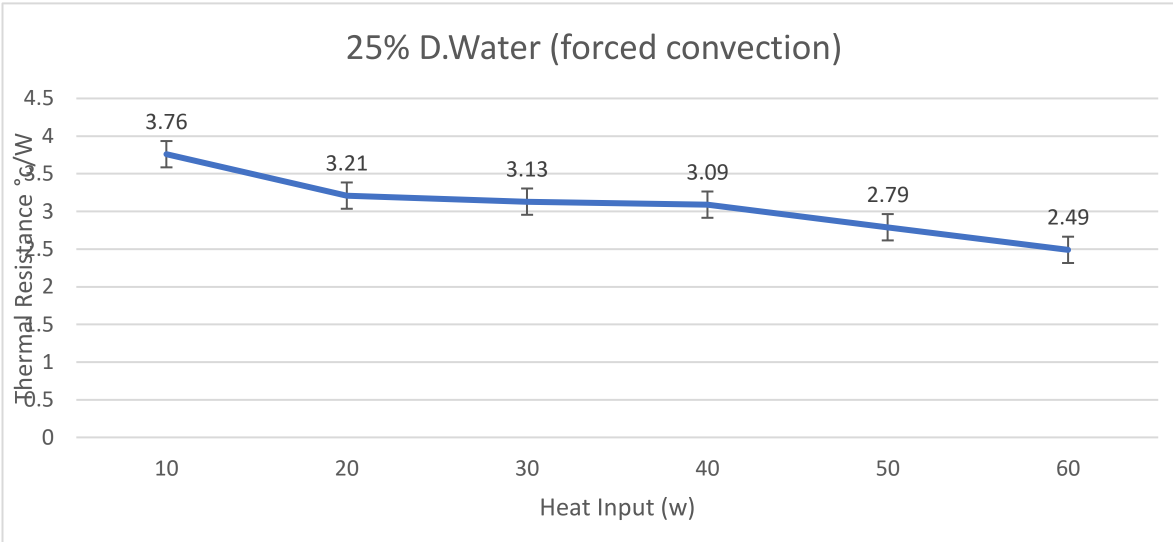

Figure 4.2.1 Thermal Resistance vs Heat input for Distilled water 25% (F. C)

In Fig. 4.2.1 It is noticed that the thermal resistance is decreasing with increment of heat input. In addition, if it is seen more closely, thermal resistance moves down in between 10W to 20W and stayed almost same up to 40W. however it decreasing gradually from 50W to 60W.

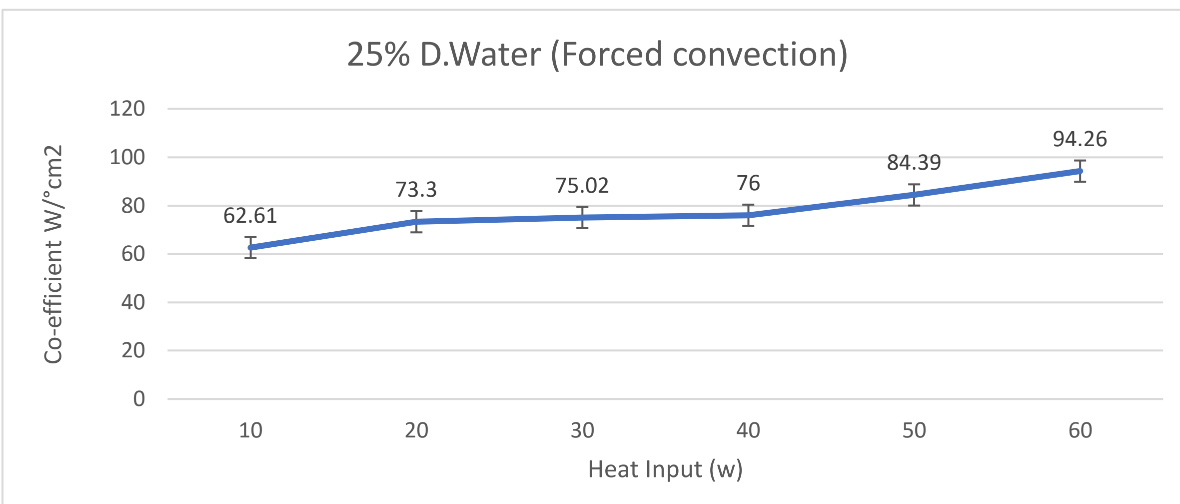

Figure 4.2.2 Thermal Co-Efficient vs Heat Input for Distilled water 25% (F. C)

In Fig. 4.2.2 It is noticed that the thermal co-efficient is increasing with decrement of heat input. In addition, if it is seen more closely, thermal co-efficient moves up in between 10W to 20W and stayed almost same up to 40W. however it increasing gradually from 50W to 60W.

4.3 Experiment conducted for DI water 50% (Natural Convection)

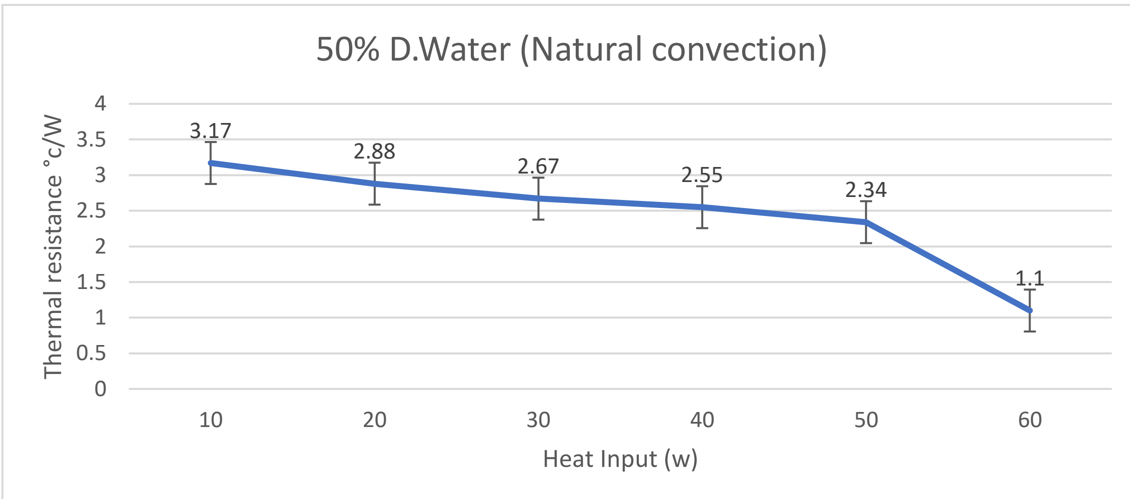

Figure 4.3.1 Thermal Resistance vs Heat input for Distilled water 50% (N. C)

In Fig. 4.3.1 It is noticed that the thermal resistance is decreasing with increment of heat input. In addition, if it is seen more closely, thermal resistance is decrease gradually from 10W to 50W. However, it goes down after that point.

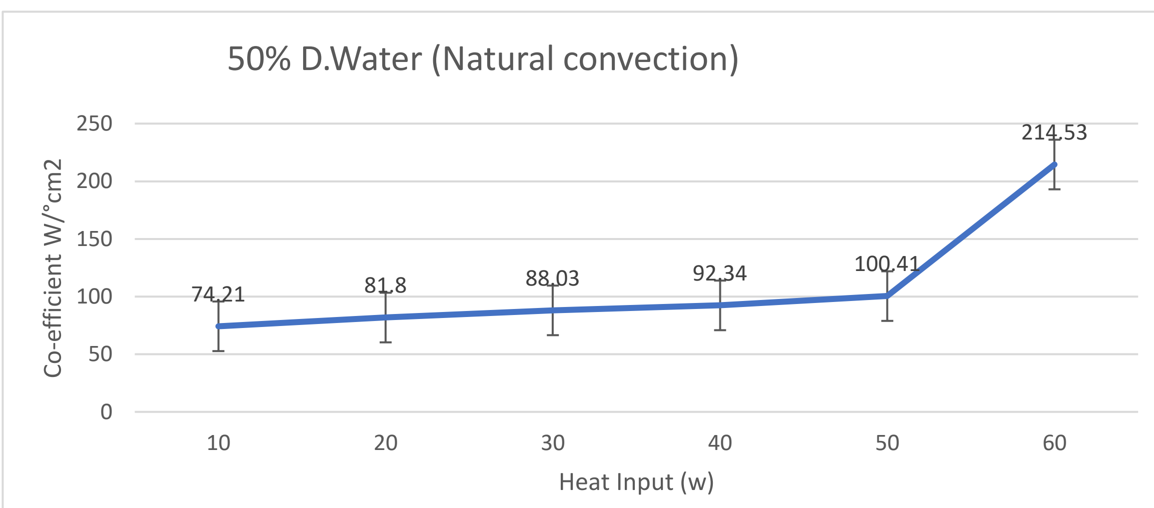

Figure 4.3.2 Thermal Co-Efficient vs Heat Input for Distilled water 50% (N. C)

In Fig. 4.3.2 It is noticed that the thermal co-efficient is increasing with decrement of heat input. In addition, if it is seen more closely, thermal co-efficient is increase gradually from 10W to 50W. However, it goes up after that point

4.4 Experiment conducted for DI water 50% (Forced Convection)

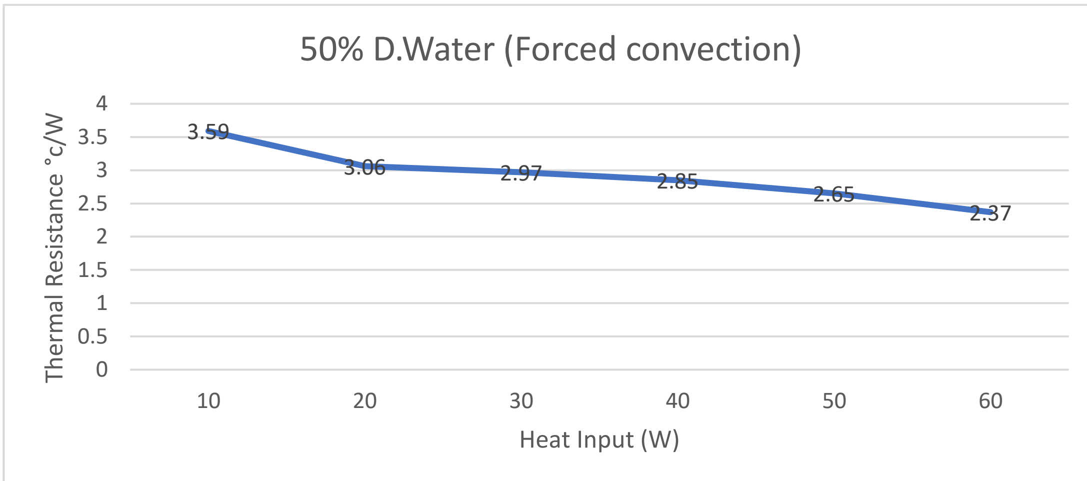

Figure 4.4.1 Thermal Resistance vs Heat input for Distilled water 50% (F. C)

In Fig. 4.4.1 It is noticed that the thermal resistance is decreasing with increment of heat input. In addition, if it is seen more closely, thermal resistance moves down in between 10W to 20W and stayed almost same up to 60W.

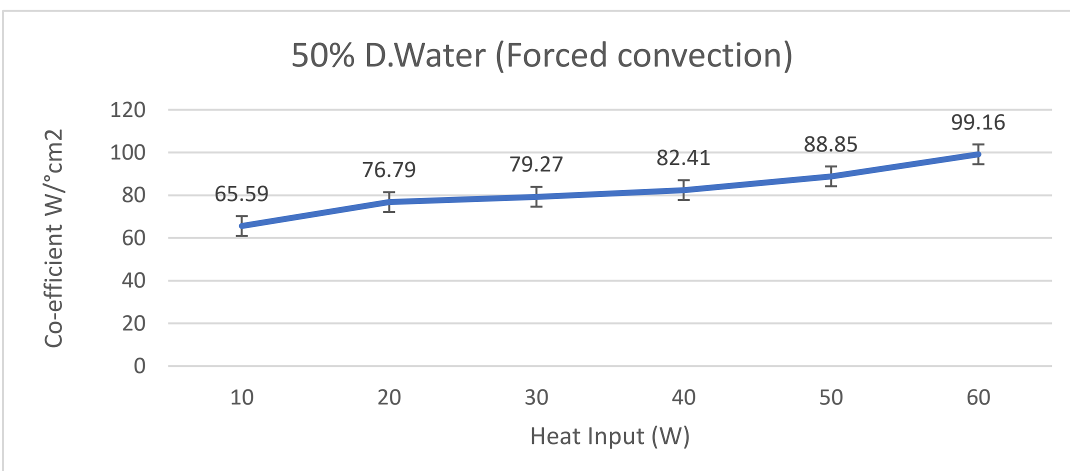

Figure 4.4.2 Thermal Co-Efficient vs Heat Input for Distilled water 50% (F. C)

In Fig. 4.4.2 It is noticed that the thermal co-efficient is increasing with decrement of heat input. In addition, if it is seen more closely, thermal co-efficient moves up in between 10W to 20W and stayed almost same up to 60W.

4.5 Experiment conducted for DI water 75% (Natural Convection)

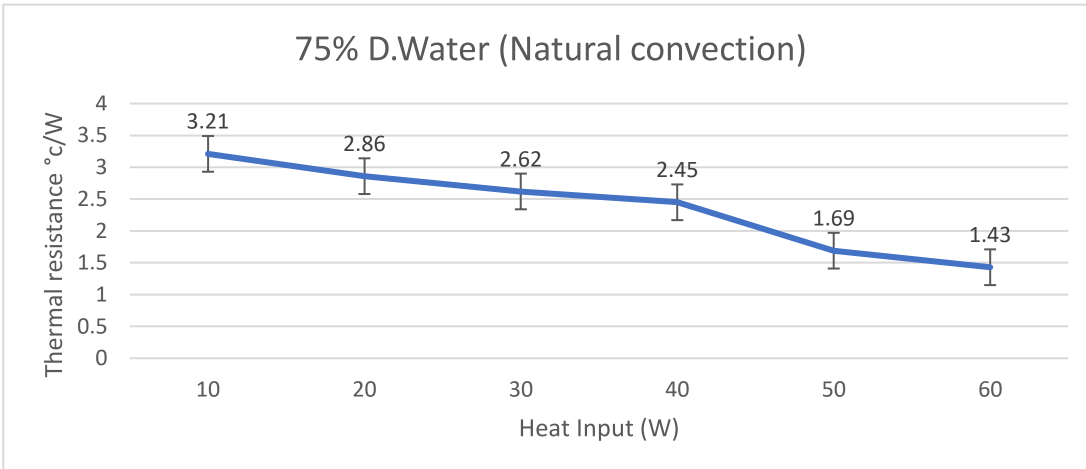

Figure 4.5.1 Thermal Resistance vs Heat Input for Distilled water 75% (N. C)

In Fig. 4.5.1 It is noticed that the thermal resistance is decreasing with increment of heat input. In addition, if it is seen more closely, thermal resistance is decreasing gradually from 10W to 40W. Then it moves down in between 400W to 50W and again up to 60W.

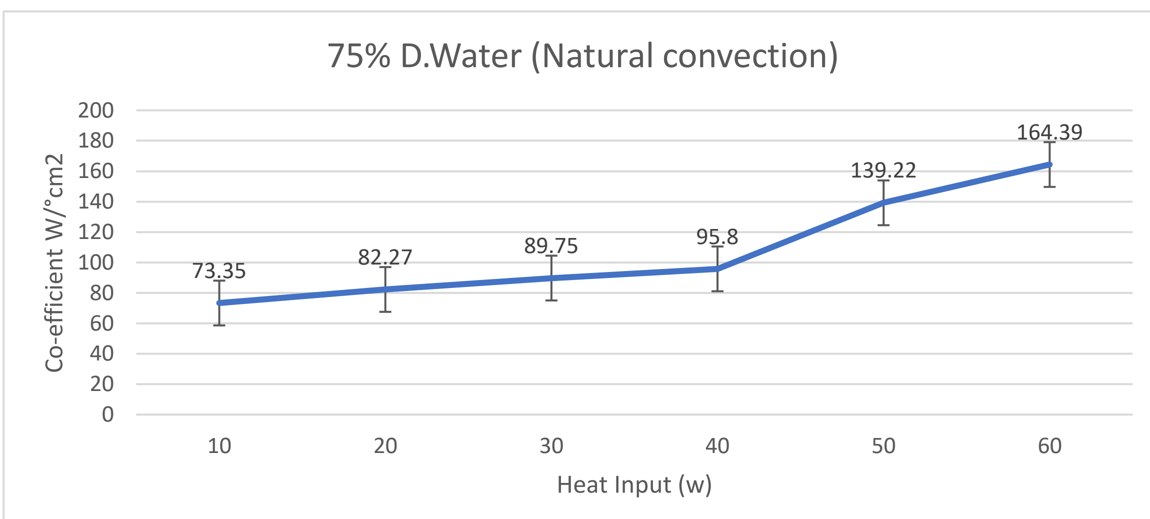

Figure 4.5.2 Thermal Co-Efficient vs Heat Input for Distilled water 75% (N. C)

In Fig. 4.5.2 It is noticed that the thermal co-efficient is increasing with decrement of heat input. In addition, if it is seen more closely, thermal co-efficient is decreasing gradually from 10W to 40W. Then it moves up in between 40W to 50W and again up to 60W.

4.6 Experiment conducted for DI water 75% (Forced Convection)

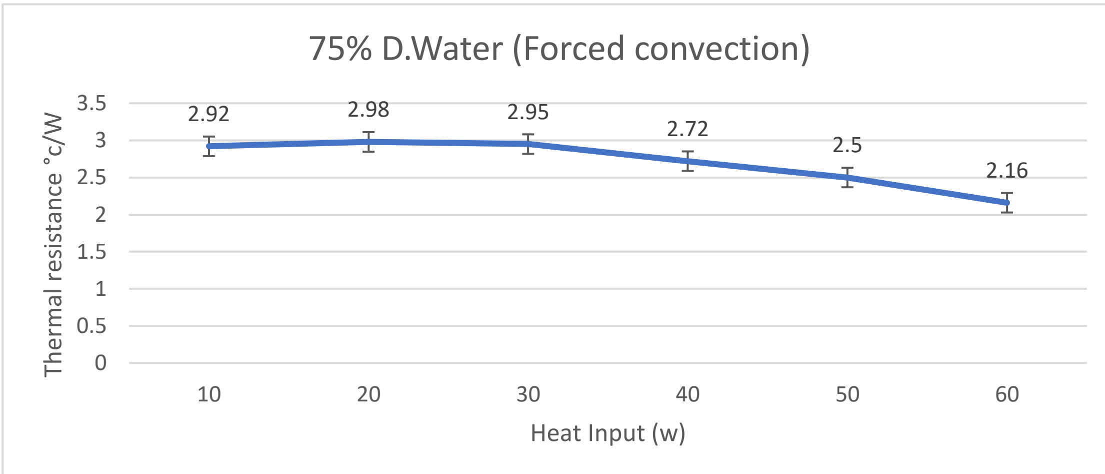

Figure 4.6.1 Thermal Resistance vs Heat Input for Distilled water 75% (F. C)

In Fig. 4.6.1 It is noticed that the thermal resistance is decreasing with increment of heat input. In addition, if it is seen more closely, thermal resistance moves up in between 10W to 20W due to started Fan. Then thermal resistance is decreasing gradually from 20W to 50W. However, it moves down after that point.

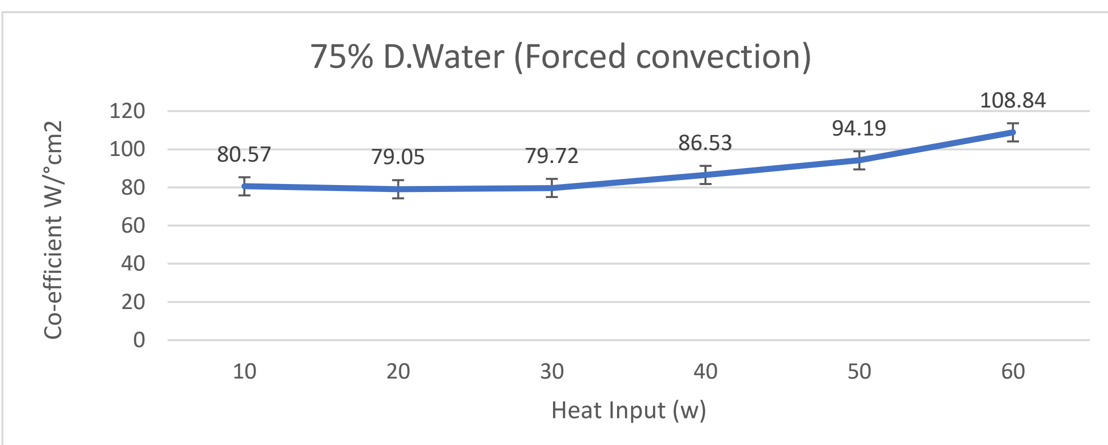

Figure 4.6.2 Thermal Co-Efficient vs Heat Input for Distilled Water 75% (F. C)

In Fig. 4.6.2 It is noticed that the thermal co-efficient is increasing with decrement of heat input. In addition, if it is seen more closely, thermal resistance moves up in between 10W to 20W due to started Fan. Then thermal co-efficient is increasing gradually from 20W to 50W. However, it moves up after that point.

4.7 Summary of Experiment conducted for DI water (Heat vs Thermal Resistance)

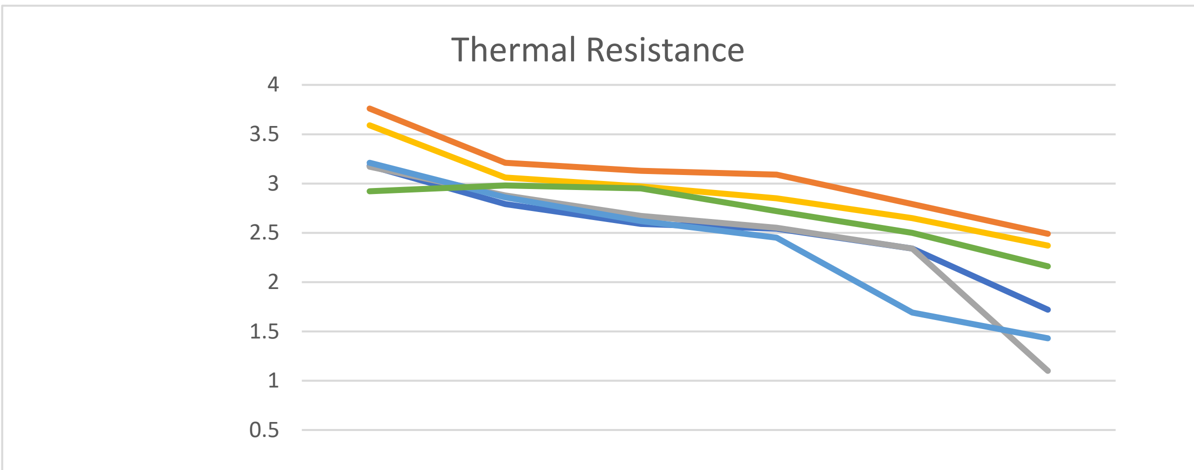

	10	20	30	40	50	60
25% D.Water N.C	3.18	2.79	2.59	2.54	2.34	1.72
25% D.Water F.C	3.76	3.21	3.13	3.09	2.79	2.49
50% D.Water N.C	3.17	2.88	2.67	2.55	2.34	1.1
50% D.Water F.C	3.59	3.06	2.97	2.85	2.65	2.37
75% D.Water N.C	3.21	2.86	2.62	2.45	1.69	1.43
75% D.Water F.C	2.92	2.98	2.95	2.72	2.5	2.16

Figure 4.7 Thermal Resistance vs Heat Input Distilled Water for all ratio

This Fig. 4.7 represent the variation of thermal resistance with heat input for different filling ratios of Water as working fluid. The fig. indicate that the thermal resistance decreases with the increase of heat input for all FR of Distilled Water. Here the lowest value of thermal resistance is obtained from 50% FR (NC). But in between 40W to 50W value of thermal resistance dramatically fall as 25% FR (NC). In this graph it is clear that, at 20W Heat input 25% of D. Water (Forced Convection) performance is better. It is also noticed that from 40W to 50W 75% of Distilled Water (Natural Convection) has better performance. Optimum performance is obtained for FR 50% (Natural convection).

4.8 Summary of Experiment conducted for DI water (Heat vs Thermal co-efficient)

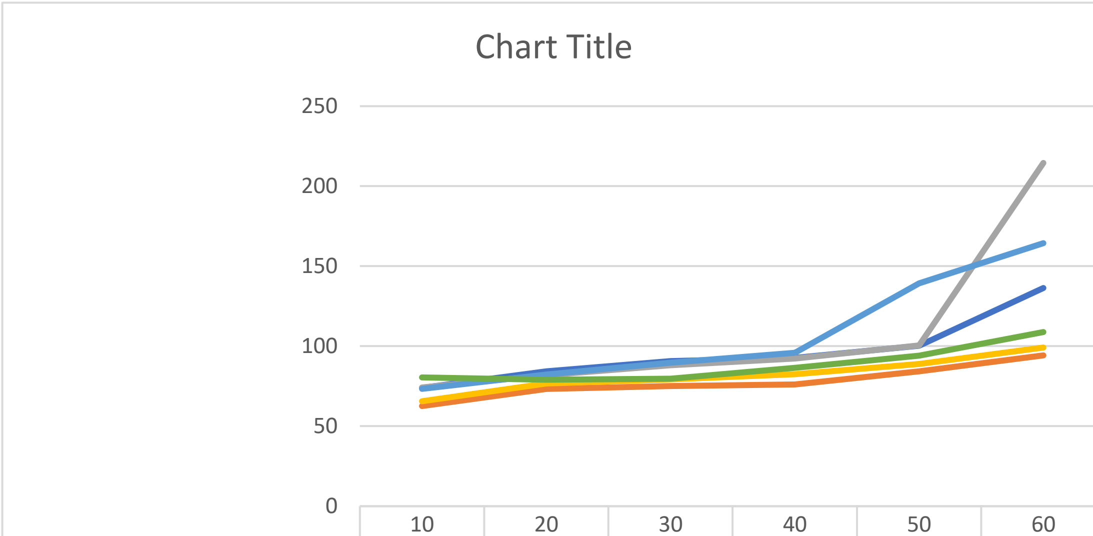

	10	20	30	40	50	60
25% D.Water N.C	73.97	84.3	90.69	92.66	100.34	136.38
25% D.Water F.C	62.61	73.3	75.02	76	84.39	94.26
50% D.Water N.C	74.21	81.8	88.03	92.34	100.41	214.53
50% D.Water F.C	65.59	76.79	79.27	82.41	88.85	99.16
75% D.Water N.C	73.35	82.27	89.75	95.8	139.22	164.39
75% D.Water F.C	80.57	79.05	79.72	86.53	94.19	108.84

Figure 4.8 Thermal Co-Efficient vs Heat Input for Distilled Water all ratio

This Fig.4.8 represent the variation of thermal co-efficient with heat input for different filling ratios of Water as working fluid. The fig. indicates that the thermal co-efficient increases with the decrease of heat input for all FR of D. Water. Here the highest value of thermal co-efficient is obtained from 50% FR (NC). But in between 40W to 50W value of thermal co-efficient is dramatically moves up as 25% FR (NC). In this graph it is clear that, at 20W Heat input 25% FR of D. Water (Forced Convection) performance is better. It is also noticed that from 40W to 50W 75% FR of D. Water (Natural Convection) has better performance. Optimum performance is obtained for FR 50% (Natural convection).

4.9 Experiment conducted for Ethanol 25% (Natural Convection)

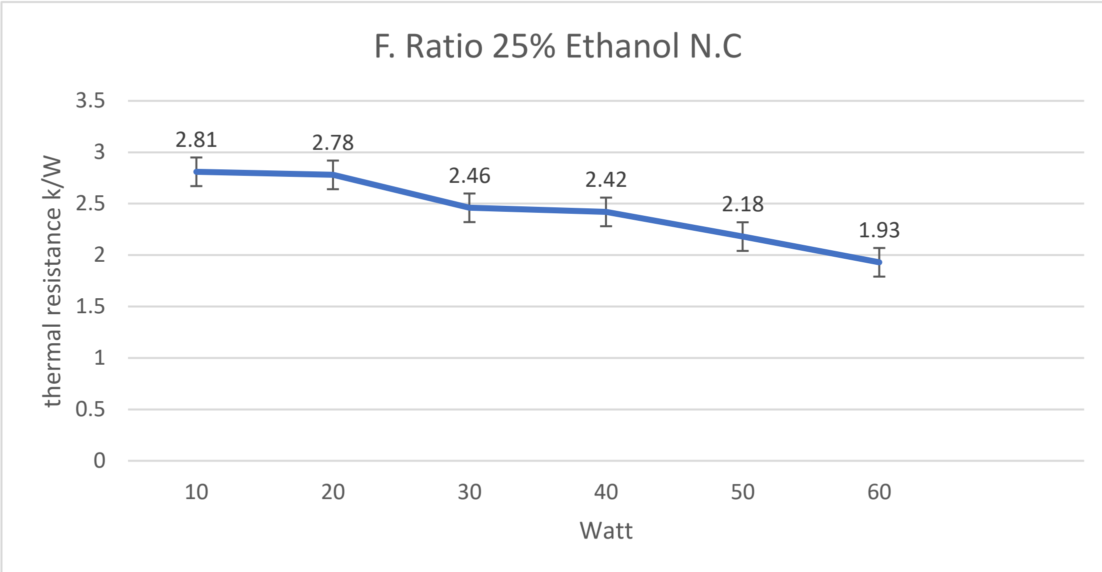

Figure 4.9.1 Thermal Resistance vs Heat Input for Ethanol 25% (N. C)

In Fig. 4.9.1, It is noticed that the thermal resistance is decreasing with increment of heat input. In addition, if it is seen more closely, thermal resistance decreasing gradually from 10W to 50W and stayed almost same after that point.

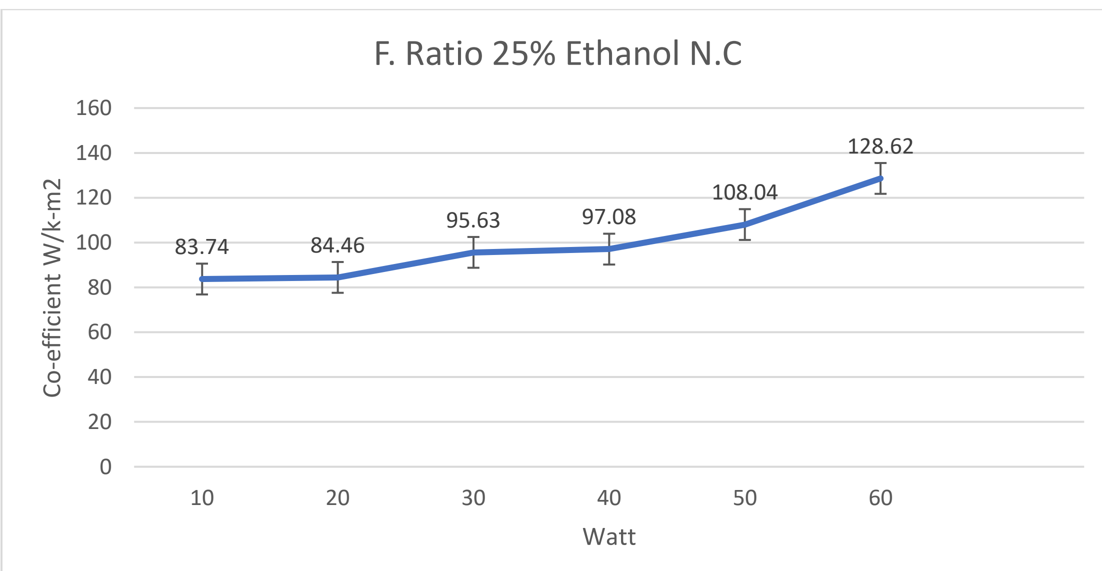

Figure 4.9.2 Thermal Co-efficient vs Heat Input for Ethanol 25% (N. C)

In Fig. 4.9.2, It is noticed that the thermal co-efficient is increasing with increment of heat input. In addition, if it is seen more closely, thermal co-efficient increasing gradually from 10W to 50W and stayed almost same after that point.

4.10 Experiment conducted for ethanol 25% (FC Convection)

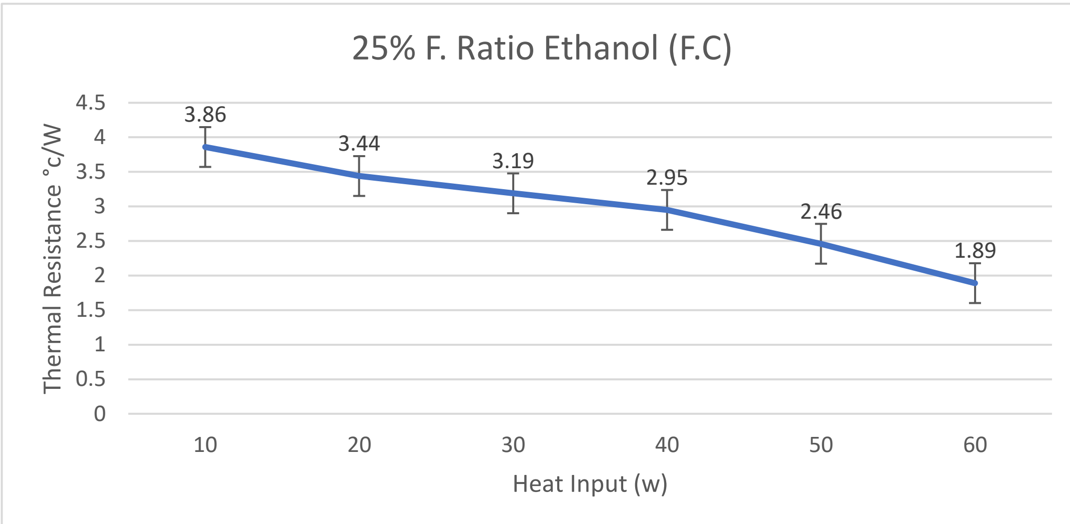

Figure 4.10.1 Thermal Resistance vs Heat Input for Ethanol 25% (F. C)

In Fig. 4.10.1 It is noticed that the thermal resistance is decreasing with increment of heat input. In addition, if it is seen more closely, thermal resistance moves down in between 10Wto 20W and stayed almost same up to 40W. However, it goes down after that point.

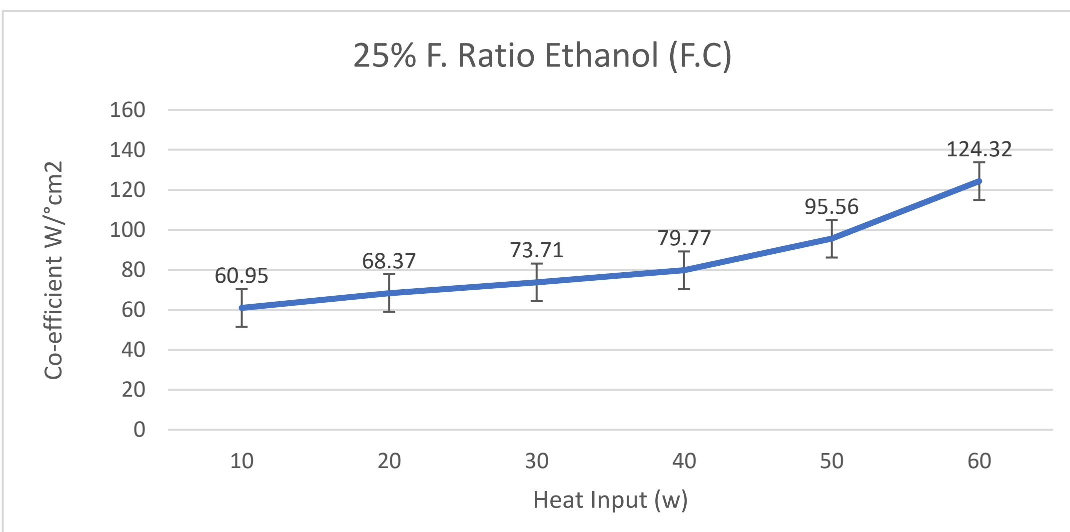

Figure 4.10.2 Thermal Co-efficient vs Heat Input for Ethanol 25% (F. C)

In Fig. 4.10.2 It is noticed that the thermal co-efficient is increasing with decrement of heat input. In addition, if it is seen more closely, thermal co-efficient moves up in between 10W to 20W and stayed almost same up to 40W. However, it goes up after that point.

4.11 Experiment conducted for ethanol 50% (Natural Convection)

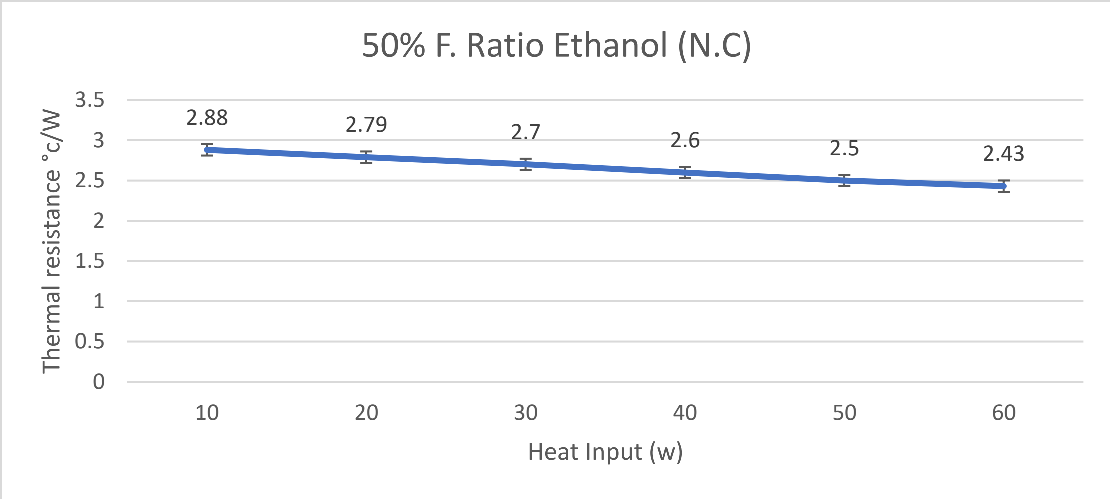

Figure 4.11.1 Thermal Resistance vs Heat Input for Ethanol 50% (N. C)

In Fig. 4.11.1 It is noticed that the thermal resistance is decreasing with increment of heat input. In addition, if it is seen more closely, thermal resistance is decreasing uniformly. In that case, steady heat transfer has been conducted.

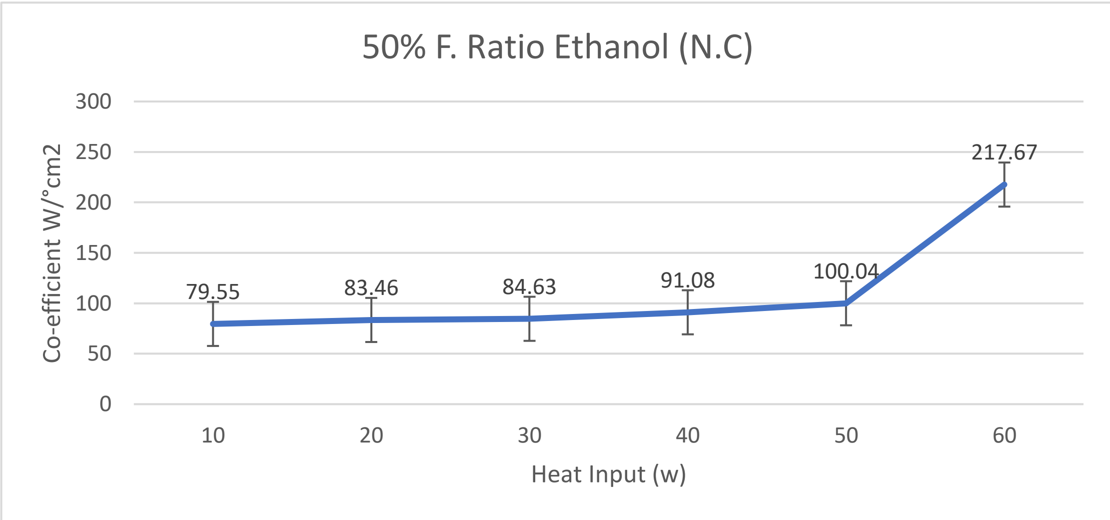

Figure 4.11.2 Thermal Co-efficient vs Heat Input for Ethanol 50% (N. C)

In Fig.4.11.2, It is noticed that the thermal co-efficient is increasing with decrement of heat input. In addition, if it is seen more closely, thermal co-efficient is increasing uniformly. However, it goes up after that point.

4.12 Experiment conducted for ethanol 50% (FC Convection)

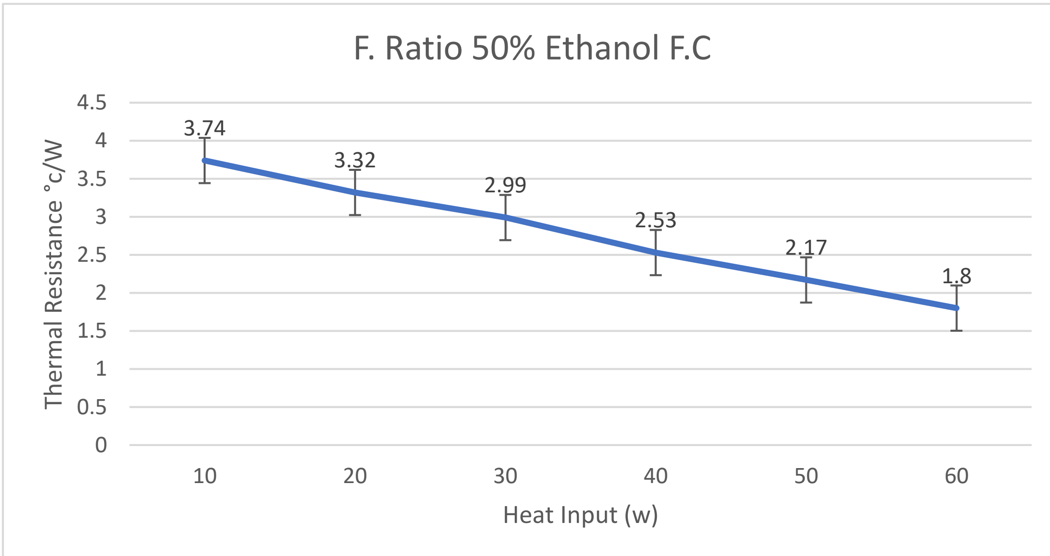

Figure 4.12.1 Thermal Resistance vs Heat Input for Ethanol 50% (F. C)

In Fig. 4.12.1 It is noticed that the thermal resistance is decreasing with increment of heat input. In addition, if it is seen more closely, thermal resistance is decreasing uniformly. In that case, steady heat transfer has been conducted.

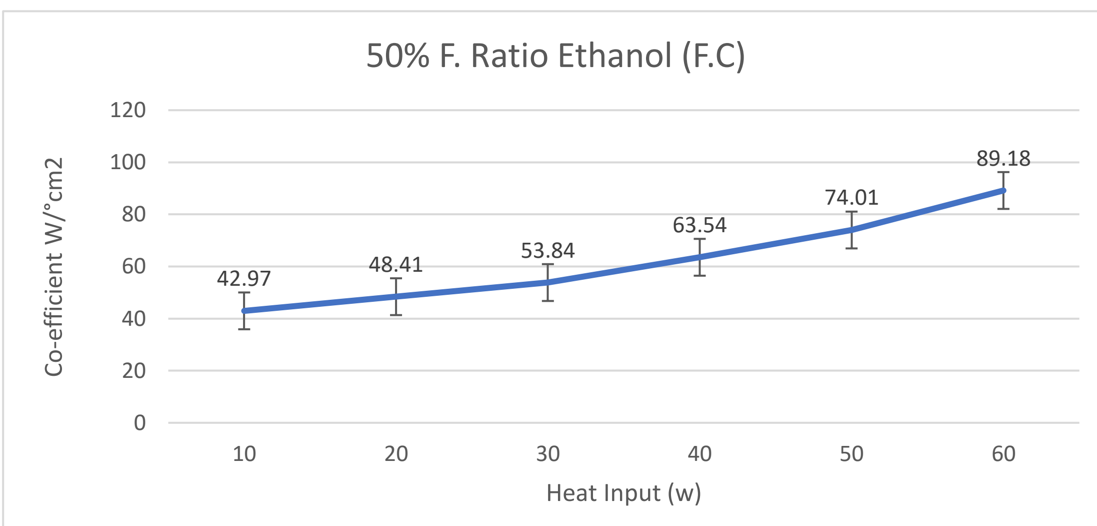

Figure 4.12.2 Thermal Co-efficient vs Heat Input for Ethanol 50% (F. C)

In Fig. 4.12.2 It is noticed that the thermal co-efficient is increasing with decrement of heat input. In addition, if it is seen more closely, thermal co-efficient increasing uniformly. In that case, steady heat transfer has been conducted.

4.13 Experiment conducted for ethanol 75% (NC Convection)

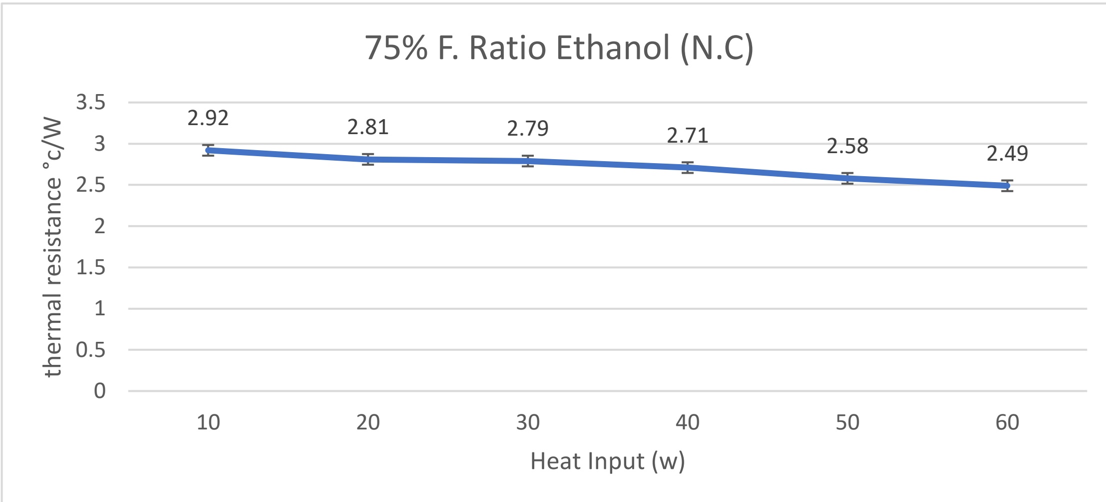

Figure 4.14.1 Thermal Resistance vs Heat Input for Ethanol 75% (N. C)

In Fig.4.13.1, It is noticed that the thermal resistance is decreasing with increment of heat input. In addition, if it is seen more closely, thermal resistance moves down in between 10W to 20W and stayed almost same up to 30W. Then it decreases from 30W to 50W gradually. However, it goes down after that point.

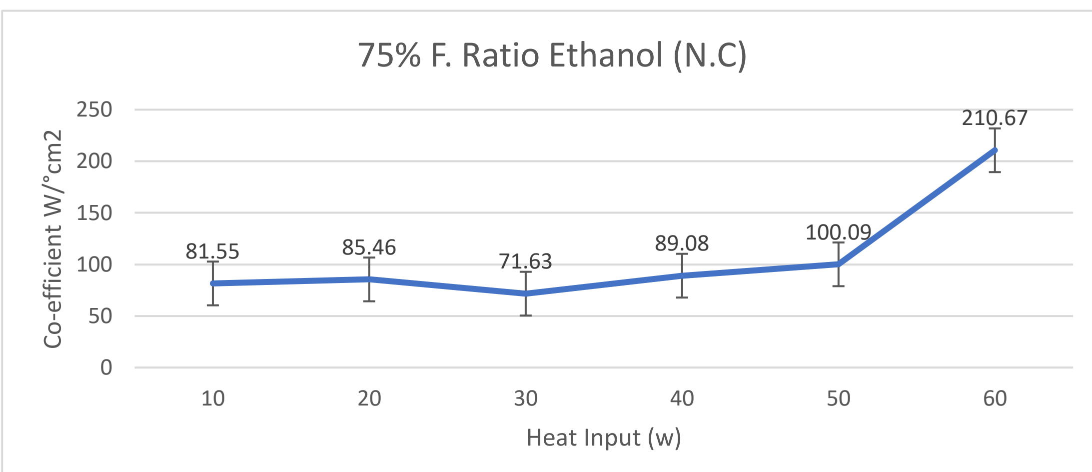

Figure 4.13.2 Thermal Co-efficient vs Heat Input for Ethanol 75% (N. C)

In Fig. 4.13.2 It is noticed that the thermal co-efficient is increasing with decrement of heat input. In addition, if it is seen more closely, thermal co-efficient moves up in between 10W to 30W and stayed almost same up to 50W. However, it goes up after that point.

4.14 Experiment conducted for ethanol 75% (Forced Convection)

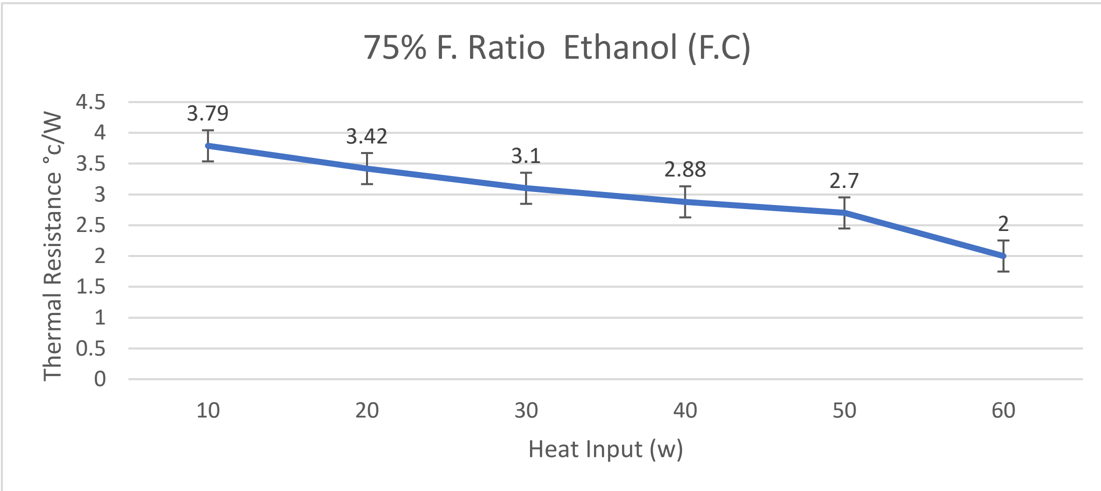

Figure 4.14.1 Thermal Resistance vs Heat Input for Ethanol 75% (F. C)

In Fig. 4.14.1 It is noticed that the thermal resistance is decreasing with increment of heat input. In addition, if it is seen more closely, thermal resistance moves down in between 10W to 40W and stayed almost same up to 50W. However, it goes down after that point.

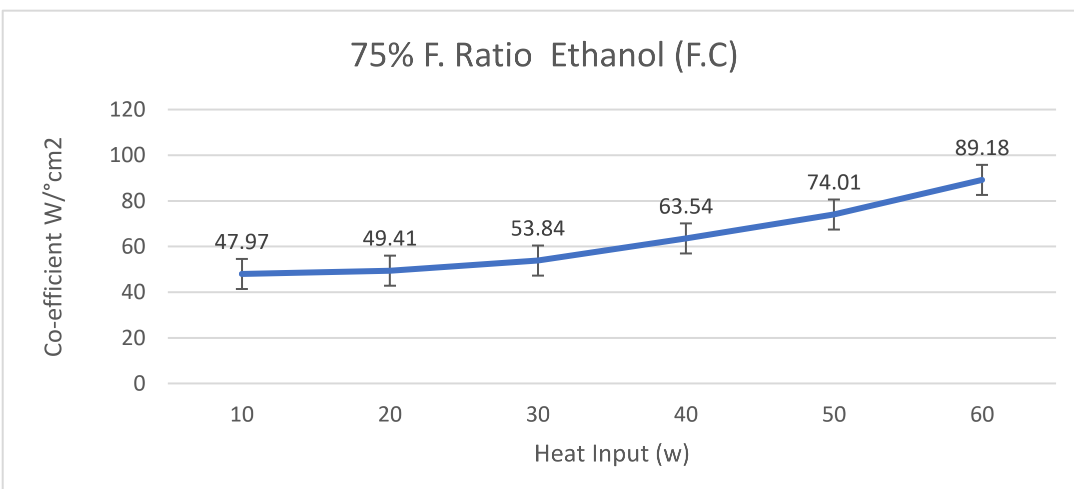

Figure 4.14.2 Thermal Co-efficient vs Heat Input for Ethanol 75% (F. C)

In Fig. 4.14.2 It is noticed that the thermal co-efficient is increasing with decrement of heat input. In addition, if it is seen more closely, thermal co-efficient moves up in between 10W to 20W and stayed almost same up to 60W.

4.15 Summary of Experiment conducted for Ethanol (Heat vs Thermal Resistance)

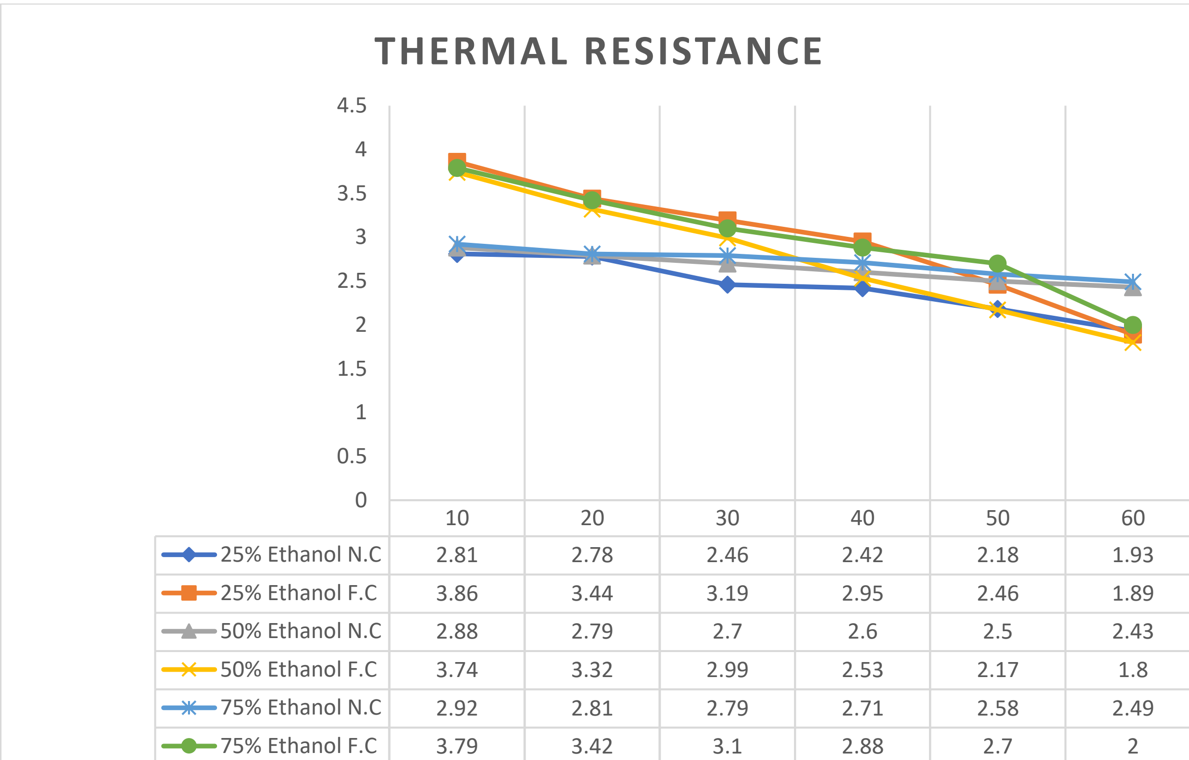

	10	20	30	40	50	60
25% Ethanol N.C	2.81	2.78	2.46	2.42	2.18	1.93
25% Ethanol F.C	3.86	3.44	3.19	2.95	2.46	1.89
50% Ethanol N.C	2.88	2.79	2.7	2.6	2.5	2.43
50% Ethanol F.C	3.74	3.32	2.99	2.53	2.17	1.8
75% Ethanol N.C	2.92	2.81	2.79	2.71	2.58	2.49
75% Ethanol F.C	3.79	3.42	3.1	2.88	2.7	2

Figure 4.15 Thermal Resistance vs Heat Input for Ethanol all ratio

This Fig. 4.15 represent the variation of thermal resistance with heat input for different filling ratios of ethanol as working fluid. The fig. indicate that the thermal resistance decreases with the increase of heat input for all filling ratio of ethanol. Here the lowest value of thermal resistance is obtained from 50% filling ratio ethanol (FC). But in between 10W to 20W, the decreasing rate of thermal resistance of 25% filling ratio ethanol (NC) and 50% filling ratio ethanol (NC) was almost same. However, it dramatically not followed by the previous rate. It goes down after 50W.

4.16 Summary of Experiment conducted for Ethanol (Heat vs Thermal coefficient)

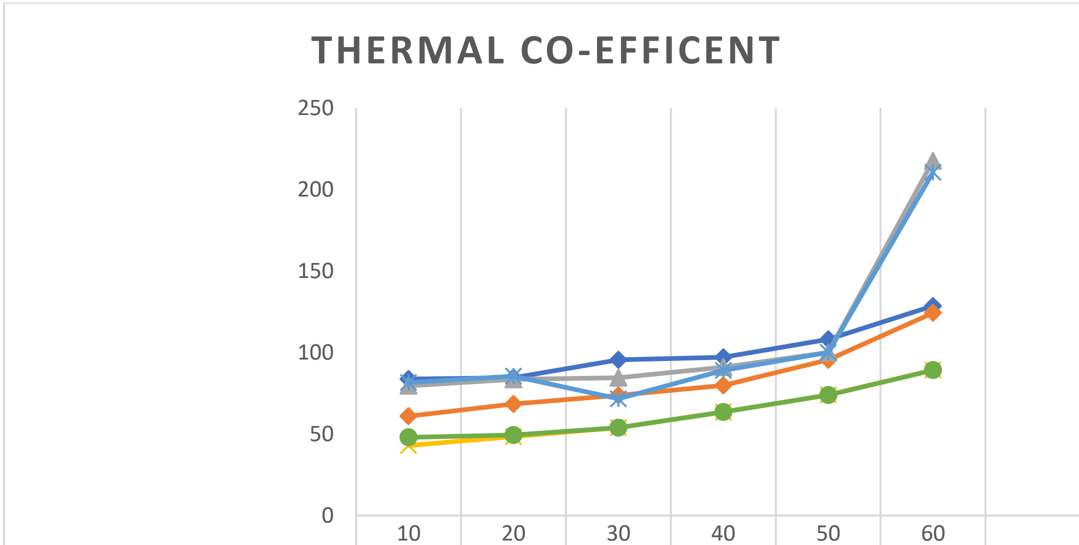

	10	20	30	40	50	60
25% Ethanol N.C	83.74	84.46	95.63	97.08	108.04	128.62
25% Ethanol F.C	60.95	68.37	73.71	79.77	95.56	124.32
50% Ethanol N.C	79.55	83.46	84.63	91.08	100.04	217.67
50% Ethanol F.C	42.97	48.41	53.84	63.54	74.01	89.18
75% Ethanol N.C	81.55	85.46	71.63	89.08	100.09	210.67
75% Ethanol F.C	47.97	49.41	53.84	63.54	74.01	89.18

Figure 4.16 Thermal Co-efficient vs Heat Input for Ethanol all ratio

This Fig.4.16 represent the variation of thermal co-efficient with heat input for different filling ratios of ethanol as working fluid. The fig. indicates that the thermal co-efficient increases with the decrease of heat input for all filling ratio of ethanol. Here the highest value of thermal co-efficient is obtained from 50% filling ratio ethanol (NC). But in between 10W to 20W, the increasing rate of thermal co-efficient of 50% filling ratio ethanol (NC) and 75% filling ratio ethanol (NC) was almost same. However, it dramatically not followed the previous rate. It goes up after 50W.

4.17 Experiment conducted for ethylene glycol 25% (Natural Convection)

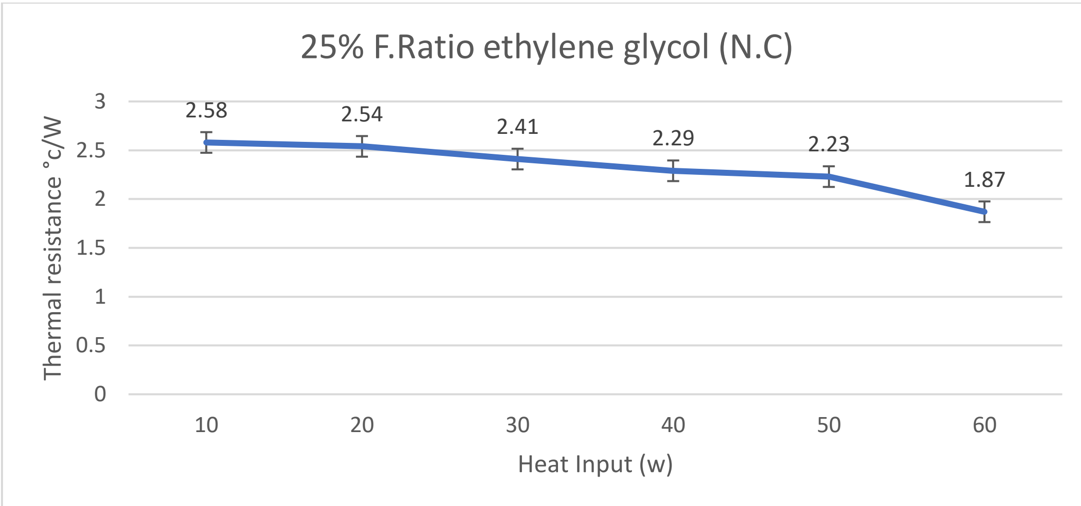

Figure 4.17.1 Thermal Resistance vs Heat Input for Ethylene Glycol 25% (N. C)

In Fig.4.17.1, It is noticed that the thermal resistance is decreasing with increment of heat input. In addition, if it is seen more closely, thermal resistance decreasing gradually from 10W to 50W. However, it goes down after that point.

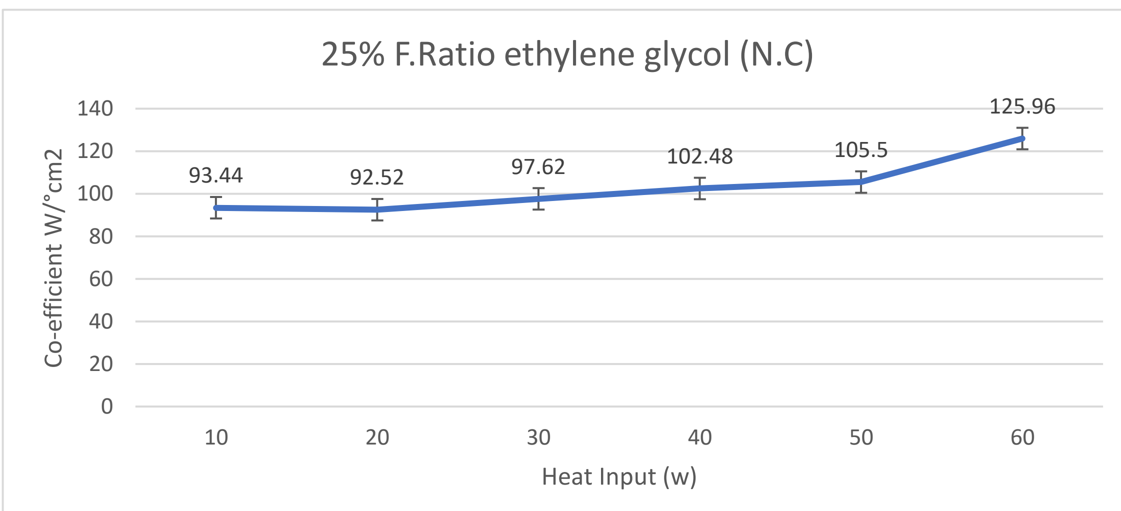

Figure 4.17.2 Thermal Resistance vs Heat Input for Ethylene Glycol 25% (N. C)

In Fig.4.17.2, It is noticed that the thermal co-efficient is increasing with increment of heat input. In addition, if it is seen more closely, thermal co-efficient increasing gradually from 10W to 50W. However, it goes up after that point.

4.18 Experiment conducted for ethylene glycol 25% (Forced Convection)

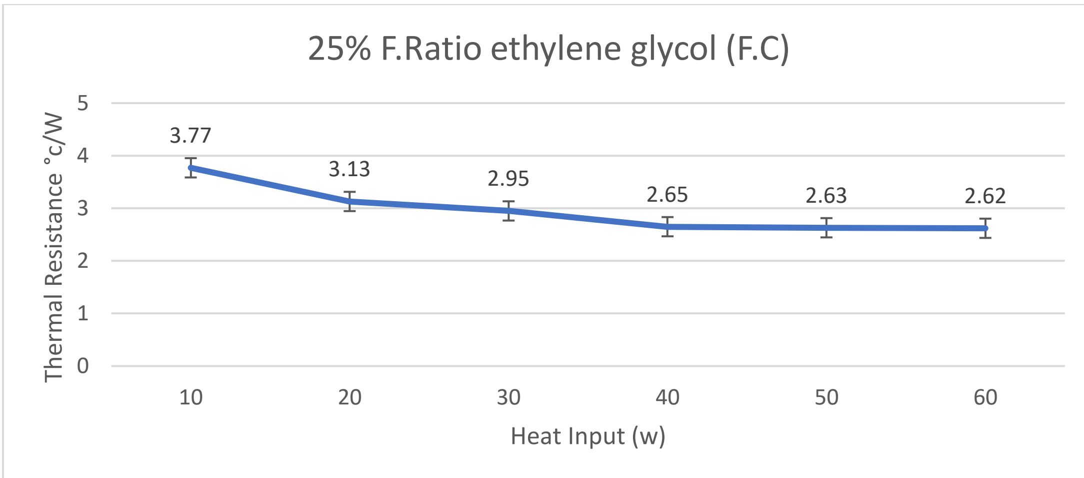

Figure 4.18.1 Thermal Resistance vs Heat Input for Ethylene Glycol 25% (F. C)

In Fig.4.18.1, It is noticed that the thermal resistance is decreasing with increment of heat input.

In addition, if it is seen more closely, thermal resistance moves down in between 10W to 20W and stayed almost same up to 60W.

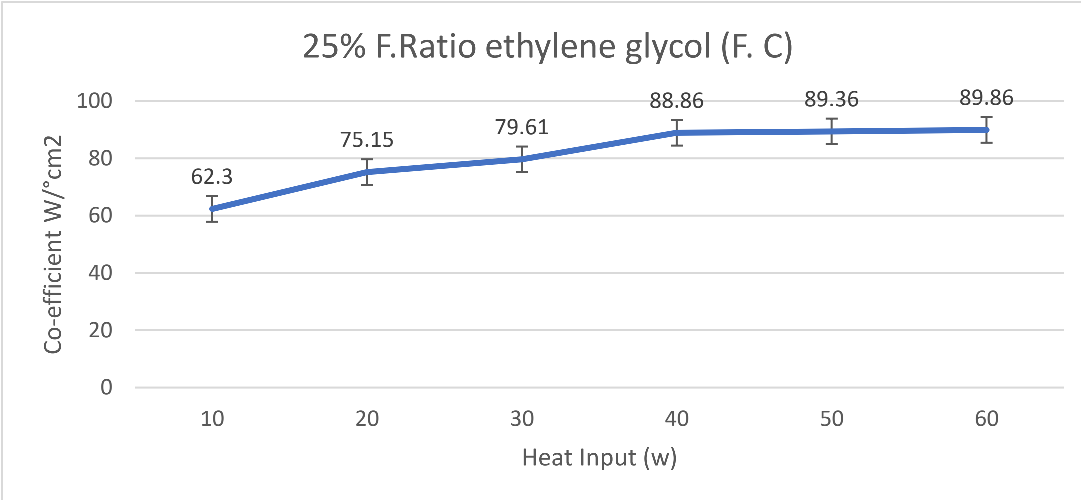

Figure 4.18.2 Thermal Co-efficient vs Heat Input for Ethylene Glycol 25% (F. C)

In Fig. 4.18.2, It is noticed that the thermal co-efficient is increasing with decrement of heat input. In addition, if it is seen more closely, thermal co-efficient up in between 10W to 20W and stayed almost same up to 60W.

4.19 Experiment conducted for ethylene glycol 50% (Natural Convection)

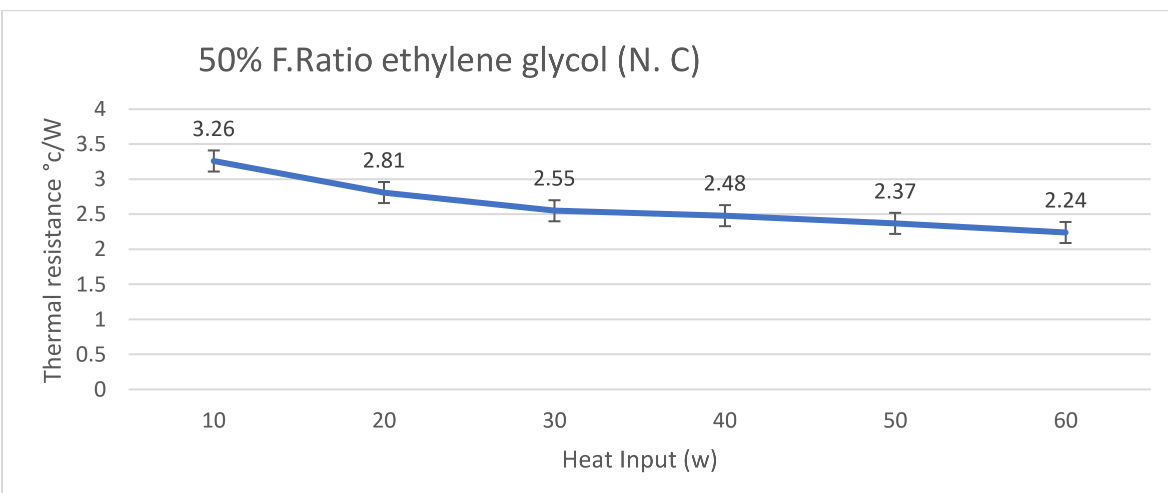

Figure 4.19.1 Thermal Resistance vs Heat Input for Ethylene Glycol 50% (N. C)

In Fig. 4.19.1, It is noticed that the thermal resistance is decreasing with increment of heat input. In addition, if it is seen more closely, thermal resistance moves down in between 10W to 30W and stayed almost same up to 60W.

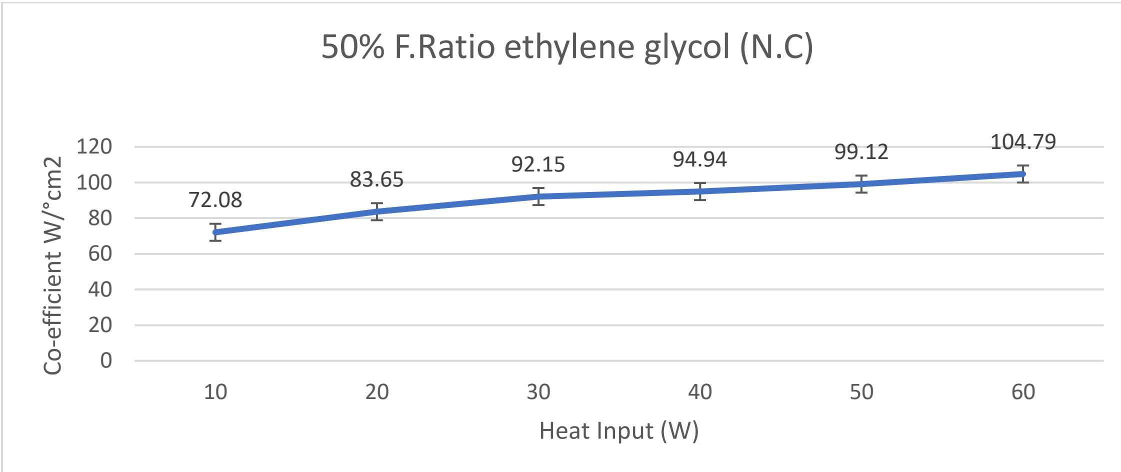

Figure 4.19.2 Thermal Co-efficient vs Heat Input for Ethylene Glycol 50% (N. C)

In Fig. 4.19.2, It is noticed that the thermal co-efficient is increasing with decrement of heat input. In addition, if it is seen more closely, thermal co-efficient moves up in between 10W to 30W and stayed almost same up to 60W.

4.20 Experiment conducted for ethylene glycol 50% (Forced Convection)

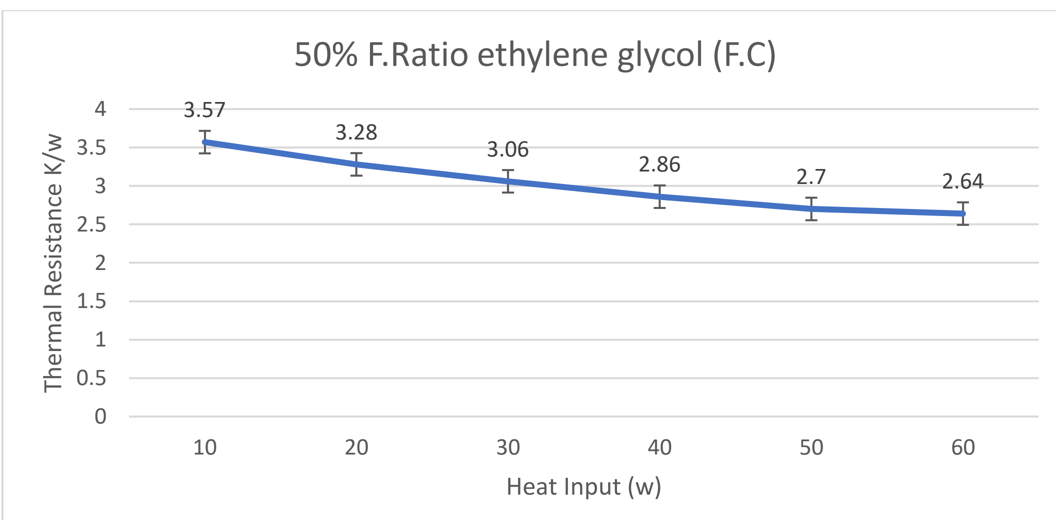

Figure 4.20.1 Thermal Resistance vs Heat Input for Ethylene Glycol 50% (F. C)

In Fig. 4.20.1, It is noticed that the thermal resistance is decreasing with increment of heat input. In addition, if it is seen more closely, thermal resistance decreases uniformly up to 60W.

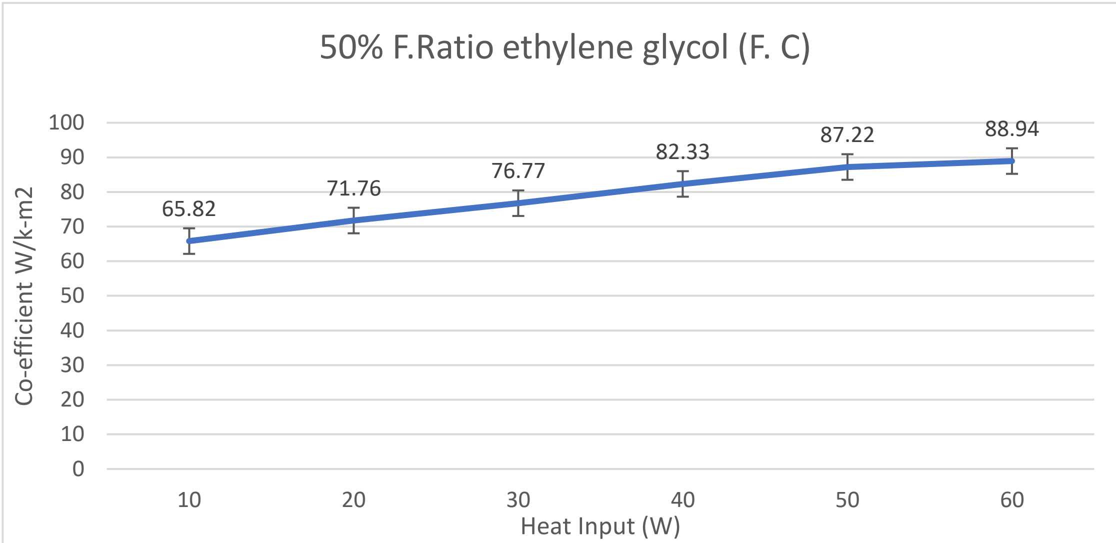

Figure 4.20.2 Thermal Co-efficient vs Heat Input for Ethylene Glycol 50% (F. C)

In Fig. 4.20.2, It is noticed that the thermal co-efficient is increasing with decrement of heat input. In addition, if it is seen more closely, thermal co-efficient increases uniformly up to 60W.

4.21 Experiment conducted for ethylene glycol 75% (Natural Convection)

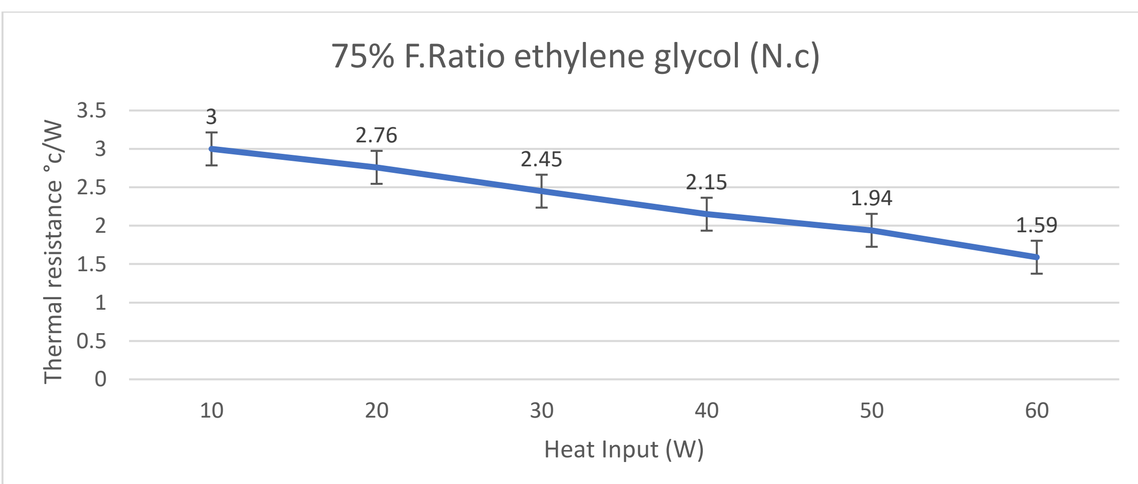

Figure 4.21.1 Thermal Resistance vs Heat Input for Ethylene Glycol 75% (N. C)

In Fig. 4.21.1, It is noticed that the thermal resistance is decreasing with increment of heat input. In addition, if it is seen more closely, thermal resistance moves down in between 10W to 30W and stayed almost same up to 50W. However, it goes down after that point.

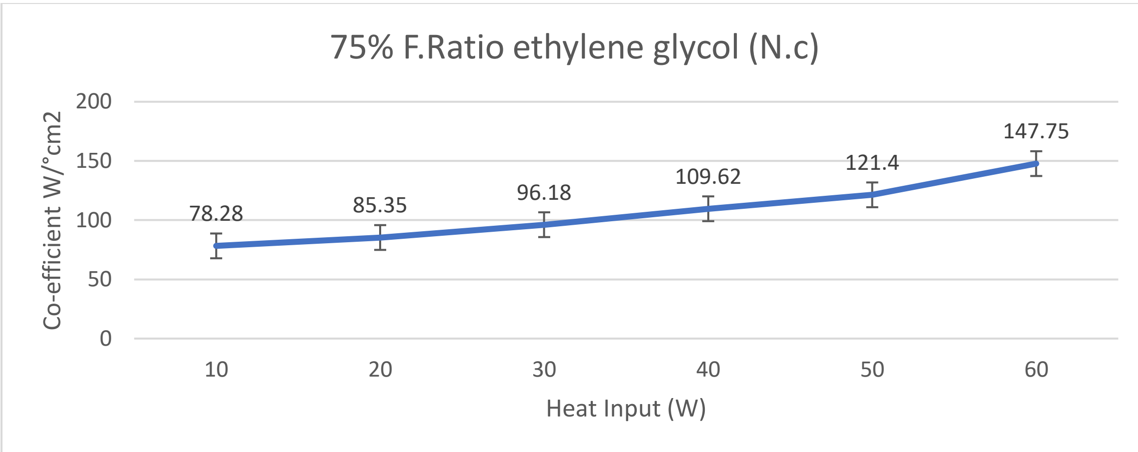

Figure 4.21.2 Thermal Co-efficient vs Heat Input for Ethylene Glycol 75% (N. C)

In Fig. 4.21.2, It is noticed that the thermal co-efficient is increasing with decrement of heat input. In addition, if it is seen more closely, thermal co-efficient moves up in between 10W to 30W and stayed almost same up to 50W. However, it goes up after that point.

4.22 Experiment conducted for ethylene glycol 75% (forced Convection)

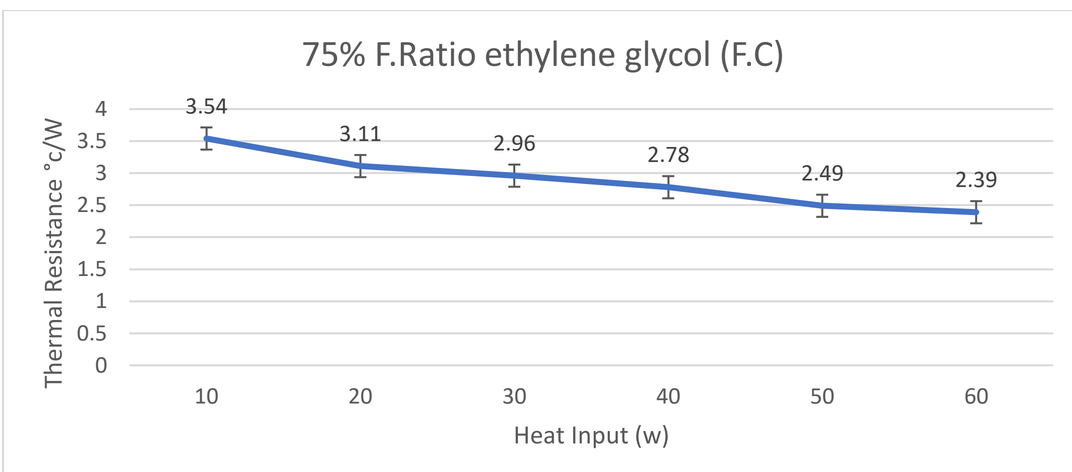

Figure 4.22.1 Thermal Resistance vs Heat Input for Ethylene Glycol 75% (F. C)

In Fig. 4.22.1, It is noticed that the thermal resistance is decreasing with increment of heat input. In addition, if it is seen more closely, thermal resistance moves down in between 10W to 20W and stayed almost same up to 60W.

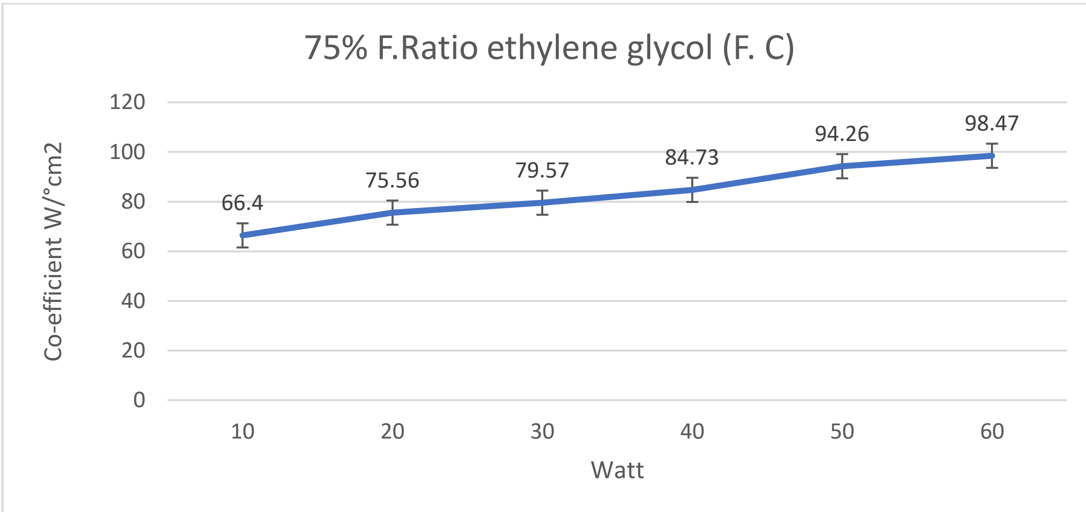

Figure 4.22.2 Thermal Co-efficient vs Heat Input for Ethylene Glycol 75% (F. C)

In Fig.4.22.2, It is noticed that the thermal co-efficient is increasing with decrement of heat input. In addition, if it is seen more closely, thermal co-efficient moves up in between 10W to 20W and stayed almost same up to 60W.

4.23 Summary of Experiment conducted for ethylene glycol (Heat vs Thermal resistance)

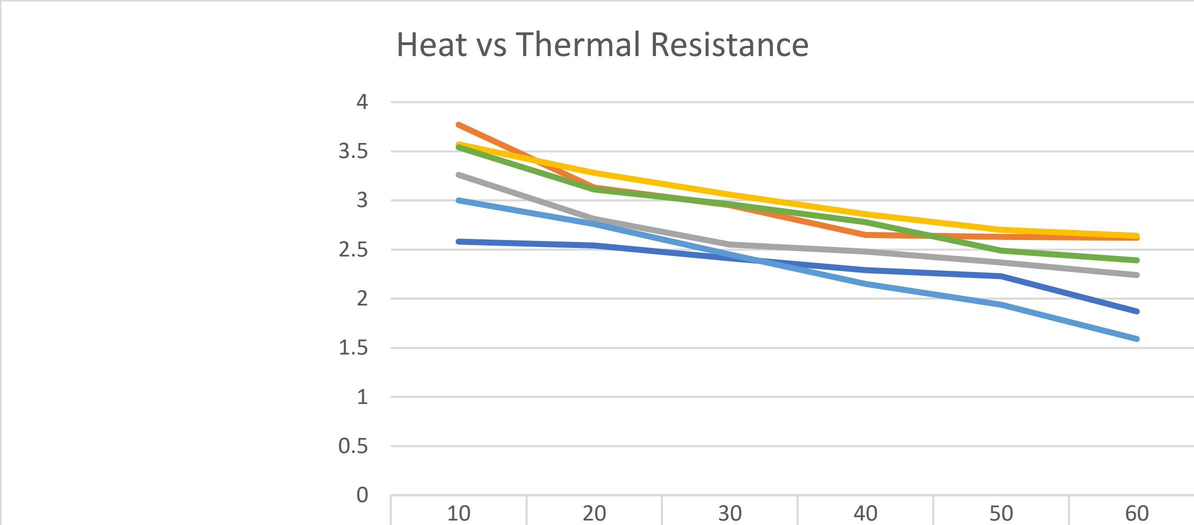

	10	20	30	40	50	60
25% Ethylene Glycol N.C	2.58	2.54	2.41	2.29	2.23	1.87
25% Ethylene Glycol F.C	3.77	3.13	2.95	2.65	2.63	2.62
50% Ethylene Glycol N.C	3.26	2.81	2.55	2.48	2.37	2.24
50% Ethylene Glycol F.C	3.57	3.28	3.06	2.86	2.7	2.64
75% Ethylene Glycol N.C	3	2.76	2.45	2.15	1.94	1.59
75% Ethylene Glycol F.C	3.54	3.11	2.96	2.78	2.49	2.39

Figure 4.1 Thermal Resistance vs Heat Input for Ethylene Glycol all ratio

This Fig. 4.23 represent the variation of thermal resistance with heat input for different filling ratios of ethylene glycol as working fluid. The fig. indicate that the thermal resistance decreases with the increase of heat input for all FR of ethylene glycol. Here the lowest value of thermal resistance is obtained from 75% FR ethylene glycol (NC). But in between 10W to 20W, the decreasing rate of thermal resistance of 25% FR ethylene glycol (NC) was high than others. However, it dramatically not followed the previous decreasing rate. It is also noticed that 50% FR of ethylene glycol (FC) has Steady decreasing rate & in between 10W to 20W heat input almost no heat transfer for 25% FR of ethylene glycol (NC).

4.24 Summary of Experiment conducted for Ethylene glycol (Heat vs Thermal coefficient)

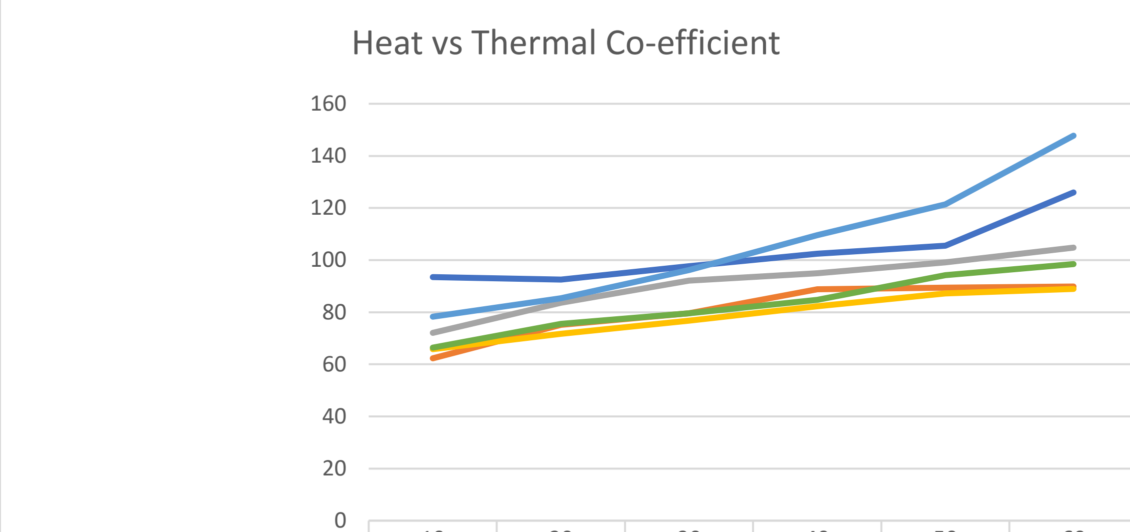

	10	20	30	40	50	60
"25% Ethylene Glycol N.C"	93.44	92.52	97.62	102.48	105.5	125.96
25% Ethylene Glycol F.C	62.3	75.15	79.61	88.86	89.36	89.86
50% Ethylene Glycol N.C	72.08	83.65	92.15	94.94	99.12	104.79
50% Ethylene Glycol F.C	65.82	71.76	76.77	82.33	87.22	88.94
75% Ethylene Glycol N.C	78.28	85.35	96.18	109.62	121.4	147.75
75% Ethylene Glycol F.C	66.4	75.56	79.57	84.73	94.26	98.47

Figure 4.2 Thermal Resistance vs Heat Input for Ethylene Glycol all ratio

This Fig. 4.24 represent the variation of thermal co-efficient with heat input for different filling ratios of ethylene glycol as working fluid. The fig. indicate that the thermal resistance increases with the decrease of heat input for all FR of ethylene glycol. Here the highest value of thermal co-efficient is obtained from 75% FR ethylene glycol (NC). But in between 10W to 20W, the increasing rate of thermal co-efficient of 25% FR ethylene glycol (NC) was low than others. However, it dramatically not followed the previous increasing rate. It is also noticed that 50% FR of ethylene glycol (FC) has Steady increasing rate & in between 10W to 20W heat input almost no heat transfer for 25% FR of ethylene glycol (NC).

4.25 Experimental Review

We experiment a close loop pulsating heat pipe and analysis the result. we use three different fluids with different ratio. Experimental results indicate that the natural convective CLPHP exhibits delayed start up pulsation and early evaporator dry out, while the forced convective CLPHP has an early start up pulsation and delayed dry out condition.

When we heated fluid, the bubbles are arranged in irregular patterns for natural convection, while active oscillations with regular bubble patterns are observed for the forced convective CLPHP. The condenser temperature affects bubble displacement, thereby leading to higher velocity for the natural convective CLPHP. The time averaged acceleration of the bubbles increases with an increase in heat transfer.

The performance of the PHPs is affected by various parameters, including its structure, working fluid, operating environment, outer diameter, number of turns, total height, filling ratio, inclination angle, and condenser area. The gravitational force also plays an important role with respect to the use of PHPs for space applications.

5 CHAPTER – CONCLUSIONS

5.1 CONCLUSIONS

The performance characteristics have been investigated on six turn closed loops pulsating heat pipe using filling ratio 25%, 50%, 75% as working fluid as D. Water, ethanol and ethylene glycol. Thermal performances has been studied by varying the heat input. Thermal Resistance and Thermal co-efficient has been calculated for all the cases and compared against each other to find the optimum performance. Based on the results obtained, the following conclusions are drawn-

I. Thermal resistance is observed to decrease with the increase of heat input for all Filling ratios of working fluids.

II. When compared to the heat inputs 10W and 20W where the temperature is continuously shooting up.

III. The filling ratio of which is liable for Optimum performance for water, ethylene glycol and ethene are 50% (NC), 75%(NC) and 25% (FC) respectively.

IV. Higher performance is obtained when F.R>50% almost

V. The performance of Natural Convection (FC) is greater than Forced Convection (FC)

Reference

[1] H. Akachi, US Patent,Patent Number 4921041, 1990.

[2] H. Akachi, Structure of micro-heat pipe,US Patent 5219020, 1993-06-15.

[3] H. Akachi, L-type heat pipe, US Patent 5490558, 1996-02-13

[4] H.Akachi, F. Polasek, P. Stulc, Pulsating heat pipes, in: Proceedings of the 5th International Heat Pipe Symposium, Melbourne, Australia, 1996, pp. 208-217.

[5] Y.Zhang and A. Faghri, "Advances and Unsolved Issues in Pulsating Heat Pipes," Heat Transfer Engineering, Vol. 29, No.1,2008, pp. 20-44. doi:I0.1080/01457630701677114.

[6] Gaugler, R. SUS patent 2350348.Appl. 21 Dec, 1972. Published 6 June 1944.and Grover, G. M US patent 3229759. Filed 1963.

[7] Rittidech S., Terdtoon P., Murakami M., Kamonpet P., Jompakdee W., Correlation to Predict Heat Transfer Characteristics of a Close-End Oscillating Heat Pipe at Normal Operating Condition, Applied Thermal Engineering, vol. 23, pp 497-510, 2003.

[8] Khandekar_PhD_Thesis_3.pdf.

[9] Honghai Yang, S. Khandekar, M. Groll, "Operational limit of closed loop pulsating heat pipes", Applied Thermal Engineering 28(2008) 49-59.

[10] S. Praful, V. P. Rao, V. Vijeth, S. v. Bhagavath, K. N. Seetharamu, and R. N. Rao, “On the operating temperature of heat pipes,” *J Phys Conf Ser*, vol. 1473, no. 1, p. 012025, Mar. 2020, doi: 10.1088/1742-6596/1473/1/012025.

[11] Y. Zhang and A. Faghri, “Heat transfer in a pulsating heat pipe with open end,” *Int J Heat Mass Transf*, vol. 45, no. 4, pp. 755–764, Dec. 2001, doi: 10.1016/S0017-9310(01)00203-4.

[12] Z. Cao, Z. Wu, M. Faghri, and B. Sundén, “Coating engineering for boiling heat transfer toward immersion cooling,” *Adv Heat Transf*, vol. 53, pp. 97–158, Jan. 2021, doi: 10.1016/bs.aiht.2021.06.002.

[13] Y. Zhang, A. Faghri, and M. B. Shafii, “Analysis of liquid-vapor pulsating flow in a U-shaped miniature tube,” *Int J Heat Mass Transf*, vol. 45, no. 12, pp. 2501–2508, Apr. 2002, doi: 10.1016/S0017-9310(01)00348-9.

[14] N. Panyoyai, P. Terdtoon and P. Sakulchangsatjatai, "Effects of Aspect Ratios and Number of Meandering Turns on Perfonnance Limit of an Inclined Closed-Loop Oscillating Heat Pipe" Energy Research Journal 2010 I (2): 91 95.

[15] P. Sakulchangsatjutai, P. Pathike and P. Terdtoon, "Effect of Length\ Ratios on Heat Transfer Characteristics of Closed-Loop Oscillating Heat Pipe with Non-Uniform Diameter" Energy.

[16] B.Y Tong close loop pulsating heat pipe at different filling ratio, 2014 IJEDR | Volume 2, Issue 2 | ISSN: 2321-9939 | IJEDR1402170.

[17-19] S. Khandekar, P. Charoensawan, M. Groll, and P. Terdtoon, “Closed loop pulsating heat pipes - Part B: Visualization and semi-empirical modeling,” *Appl Therm Eng*, vol. 23, no. 16, pp. 2021–2033, Nov. 2003, doi: 10.1016/S1359-4311(03)00168-6.

Appendix -1

Calculation of filling ratio

Let,

V = Internal volume of the heat pipe

= 100 % Fill Ratio

A = Area of heat pipe

L = Total length of heat pipe

Now, V = $(\pi \times D_i^2 \times L)/4$ mm^3

= $(3.1416\times2^2\times2855)/4$ mm^3

= 8969.268 mm^3

≈ 8.969 ml

= 9 ml

As there is no additional container for working fluid in the test setup, the total internal volume of the pipe is considered to be the maximum capacity of the system. For example, to study the heat transfer characteristics 2.25 ml, 4.5 ml and 6.8 ml of working fluids were used which yielded 25%, 50% and 75% filling ratio respectively.

Calculation of Thermal Resistance

T_e = Average temperature of evaporation

T_c = Average temperature of condenser

$\Delta t = T_e - T_c$

Let, R_{th} = Thermal Resistance

= $\Delta t/Q$

= $(T_e - T_c)/Q$ $^oC/W$

Calculation of Co-Efficient

Let, h = Heat transfers co-efficient

$$= \frac{Q}{A_e(\Delta T)} \text{ W/C-}m^2$$

$$=\frac{Q}{A_e(T_{e-T_c})}\ \text{W/C-}m^2$$

Now A_e = π × 2.75 × (12×50) [6 turns = 12 CLPHP 50mm evaporator] mm^2

Appendix-2

Collected data for experiment

Table 3 Experiment Data for DI water 25% Natural Convection

Log Time (Sec)	Resistance	Co-efficient	Watt
600	3.18	73.97	10
600	2.79	84.3	20
600	2.59	90.69	30
601	2.54	92.66	40
600	2.34	100.34	50
601	1.72	136.38	60

Table 4 Experiment Data for DI water 25% Forced Convection

Log Time (Sec)	Resistance	Co-efficient	Watt
600	3.76	62.61	10
600	3.21	73.3	20
600	3.13	75.02	30
600	3.09	76	40
601	2.79	84.39	50
600	2.49	94.26	60

Table 5 Experiment Data for DI water 50% Natural Convection

Log Time (Sec)	Resistance	Co-efficient	Watt
600	3.17	74.21	10
600	2.88	81.8	20
600	2.67	88.03	30
601	2.55	92.34	40
600	2.34	100.41	50
601	1.1	214.53	60

Table 5 Experiment Data for DI water 50% Forced Convection

Log Time (Sec)	Resistance	Co-efficient	Watt
600	3.59	65.59	10
600	3.06	76.79	20
600	2.97	79.27	30
600	2.85	82.41	40
601	2.65	88.85	50
601	2.37	99.16	60

Table 6 Experiment Data for DI water 75% Natural Convection

Log Time (Sec)	Resistance	Co-efficient	Watt
600	3.21	73.35	10
600	2.86	82.27	20
600	2.62	89.75	30
601	2.45	95.8	40
600	1.69	139.22	50
600	1.43	164.39	60

Table 7 Experiment Data for DI water 75% Forced Convection

Log Time (Sec)	Resistance	Co-efficient	Watt
600	2.92	80.57	10
600	2.98	79.05	20
600	2.95	79.72	30
600	2.72	86.53	40
600	2.5	94.19	50
601	2.16	108.84	60

Table 8 Experiment Data for Ethanol 25% Natural Convection

Log Time (Sec)	Resistance	Co-efficient	Watt
600	2.81	83.74	10
600	2.78	84.46	20
600	2.46	95.63	30
601	2.42	97.08	40
600	2.18	108.04	50
601	0.74	317.67	60

Table 9 Experiment Data for Ethanol 25% Forced Convection

Log Time (Sec)	Resistance	Co-efficient	Watt
600	3.86	60.95	10
600	3.44	68.37	20
600	3.19	73.71	30
600	2.95	79.77	40
601	2.46	95.56	50
601	1.89	124.32	60

Table 10 Experiment Data for Ethanol 50% Natural Convection

Log Time (Sec)	**Resistance**	**Co-efficient**	**Watt**
600	2.88	79.55	10
600	2.79	83.46	20
600	2.7	84.63	30
601	2.6	91.08	40
600	2.5	100.04	50
601	2.43	217.67	60

Table 11 Experiment Data for Ethanol 50% Forced Convection

Log Time (Sec)	**Resistance**	**Co-efficient**	**Watt**
602	3.74	42.97	10
601	3.32	48.41	20
602	2.99	53.84	30
602	2.53	63.54	40
602	2.17	74.01	50
603	1.8	89.18	60

Table 12 Experiment Data for Ethanol 75% Natural Convection

Log Time (Sec)	**Resistance**	**Co-efficient**	**Watt**
600	2.92	81.55	10
600	2.81	85.46	20
600	2.79	71.63	30
601	2.71	89.08	40
600	2.58	100.09	50
601	2.49	210.67	60

Table 13 Experiment Data for Ethanol 75% Forced Convection

Log Time (Sec)	**Resistance**	**Co-efficient**	**Watt**
602	3.79	47.97	10
601	3.42	49.41	20
602	3.1	53.84	30
602	2.88	63.54	40
602	2.7	74.01	50
603	2	89.18	60

Table 14 Experiment Data for Ethylene Glycol 25% Natural Convection

Log Time (Sec)	**Resistance**	**Co-efficient**	**Watt**
600	2.58	93.44	10
600	2.54	92.52	20
600	2.41	97.62	30
601	2.29	102.48	40
600	2.23	105.5	50
600	1.87	125.96	60

Table 15 Experiment Data for Ethylene Glycol 25% Forced Convection

Log Time (Sec)	Resistance	Co-efficient	Watt
600	3.77	62.3	10
600	3.13	75.15	20
600	2.95	79.61	30
600	2.65	88.86	40
601	2.63	89.36	50
600	2.62	89.86	60

Table 16 Experiment Data for Ethylene Glycol 50% Natural Convection

Log Time (Sec)	Resistance	Co-efficient	Watt
600	3.26	72.08	10
600	2.81	83.65	20
600	2.55	92.15	30
601	2.48	94.94	40
601	2.37	99.12	50
600	2.24	104.79	60

Table 17 Experiment Data for Ethylene Glycol 50% Forced Convection

Log Time (Sec)	Resistance	Co-efficient	Watt
600	3.57	65.82	10
600	3.28	71.76	20
600	3.06	76.77	30
600	2.86	82.33	40
601	2.7	87.22	50
600	2.64	88.94	60

Table 18 Experiment Data for Ethylene Glycol 75% Natural Convection

Log Time (Sec)	Resistance	Co-efficient	Watt
600	3	78.28	10
600	2.76	85.35	20
600	2.45	96.18	30
601	2.15	109.62	40
600	1.94	121.4	50
601	1.59	147.75	60

Table 19 Experiment Data for Ethylene Glycol 75% Forced Convection

Log Time (Sec)	Resistance	Co-efficient	Watt
600	3.54	66.4	10
600	3.11	75.56	20
600	2.96	79.57	30
600	2.78	84.73	40
600	2.49	94.26	50
600	2.39	98.47	60